Received: 2 October 2020 | Revised: 18 January 2021 | Accepted: 18 January 2021

DOI: 10.1002/gj.4091

RESEARCH ARTICLE

WILEY

Impact of petrographic characteristics on reservoir quality of tight sandstone reservoirs in coal-bearing strata: A case study in Lower Permian Shihezi Formation in northern Ordos Basin, China

Zihao Liu[1,2] | Shenghe Wu[1,2] | Jinbu Li[3] | Zhenhua Xu[1,2] | Miao Tian[1,2] | Tianyou Zhang[1,2] | Yang An[4]

[1]State Key Laboratory of Petroleum Resources and Prospecting, China University of Petroleum, Beijing, China

[2]College of Geosciences, China University of Petroleum, Beijing, China

[3]Research Institute of Exploration and Development, Changqing Oilfield Company, PetroChina, Xi'an, China

[4]Research Institute of Exploration and Development, Daqing Oilfield Company, PetroChina, Daqing, China

Correspondence
Shenghe Wu, State Key Laboratory of Petroleum Resources and Prospecting, China University of Petroleum, Beijing 102249, China.
Email: reser@cup.edu.cn

Funding information
Major National Science and Technology Projects of China, Grant/Award Number: 2017ZX05009001; The National Natural Science Foundation of China, Grant/Award Number: No. 41772101

Handling Editor: I. Somerville

The lower Shihezi Formation in the Sulige gas field is the main gas exploitation target in the Ordos Basin and is crucial in finding high-quality reservoirs for further exploration. Using X-ray diffraction, cathodoluminescence (CL), and scanning electron microscope (SEM) techniques, the eighth member of lower Shihezi Formation (He8) sandstones are characterized as fine- to coarse-grained quartzarenite and litharenite with good sorting, which are controlled by different sources and depositional faces. Four types of sandstones are recognized according to varied petrographic characteristics, among which fine-grained sandstones (type I) has the poorest reservoir quality and coarse-grained sandstones with chlorite coating (type II) are the best reservoirs. The complicated diagenetic process mainly includes intense compaction, two-stage dissolution, quartz and calcite cementation, which is closely associated with the thermal evolution of coals. The increased ductile fragments account for low reservoir quality in type I sandstones. Due to the absence of feldspar, the influence of other detrital components on the reservoir quality has increased. Sandstones with abundant volcanic fragments (type II) usually formed grain-coating chlorite, which inhibit tight compaction and quartz cementations. Quartz overgrowth originated from feldspar dissolution as well as pressure dissolution of detrital quartz are frequently observed in medium- to coarse-grained quartzarenite (type III). The high-quality reservoir exits when the ductile grains content is about 4%, according to the negative relationship between quartz cement and ductile content. Although there are a lot of dissolution pores in medium- to coarse-grained litharenite (type IV), the reservoir quality did not improve much due to the diagenetic minerals filling in the secondary pores.

KEYWORDS
coal-bearing strata, diagenesis, Ordos Basin, petrographic characteristics, quartz cementation, tight gas reservoir

1 | INTRODUCTION

Tight sandstone reservoirs in coal-bearing strata are gradually receiving much interest because of their large hydrocarbon reserves worldwide (Zou et al., 2012). In China, the production of gas in coal buried strata has reached 902×10^8 m^3, accounting for 61.5% of the total production (Zou et al., 2019). Therefore, it is very significant to focus on factors affecting production in coal buried tight sandstones.

Reservoir quality has been proved to be the critical factor during hydrocarbon exploration in tight sandstone reservoirs (Lai et al., 2018; Li et al., 2019; Morad, Al-Ramadan, Ketzer, & De Ros, 2010). Meanwhile, petrographic characteristics have appreciable impact on reservoir qualities, and their variation in space causes reservoir heterogeneity horizontally and vertically (Bjørlykke, 2014; Li, Chang, Yin, Sun, & Song, 2017; Rahman & Worden, 2016; Tian, Omre, & Xu, 2020; Wang, Chang, Yin, Li, & Song, 2017). Petrographic characteristics are mainly controlled by sources and sedimentary facies, and factors like grain size, sorting, and detrital composition play an important role on compaction, diagenetic alteration, and dissolution, leading to variations in reservoir qualities (Bjørlykke, 2014; Chuhan, Kjeldstad, Bjørlykke, & Høeg, 2002, 2003; Fan, Yang, Li, Zhao, & Van Loon, 2017; Liu, Hu, Cao, Wang, & Tang, 2018; Wang et al., 2017; Yang & Liu, 2014).

However, unlike other source rocks, thermal evolution of coal is more complex, with more acid fluid released into sandstone reservoirs (Hou, Zhu, Chen, Wang, & Liu, 2020; Shuai et al., 2013). The absence of early calcite cement, as well as large amounts of feldspar dissolution and quartz cementation, has been typical characteristics of tight sandstones in coal-bearing strata (Hou et al., 2020; Yu et al., 2019), where the impact of texture and detrital composition on reservoir quality can be very different. Previous studies have paid much attention on how coal evolution affects diagenetic process of sandstones, while the impact of petrographic characteristics on reservoir quality during the process is not well understood. The relationships among petrographic characteristics, diagenesis, and reservoir quality of tight sandstones in coal-bearing strata are still not clear.

The Sulige gas field is currently the largest and most typical coal-bearing tight sandstone gas field in China (Zou et al., 2019). In Sulige gas field, the eighth member of lower Permian Shihezi Formation (He8) is the main gas productive layer (Fan et al., 2019). Plenty of

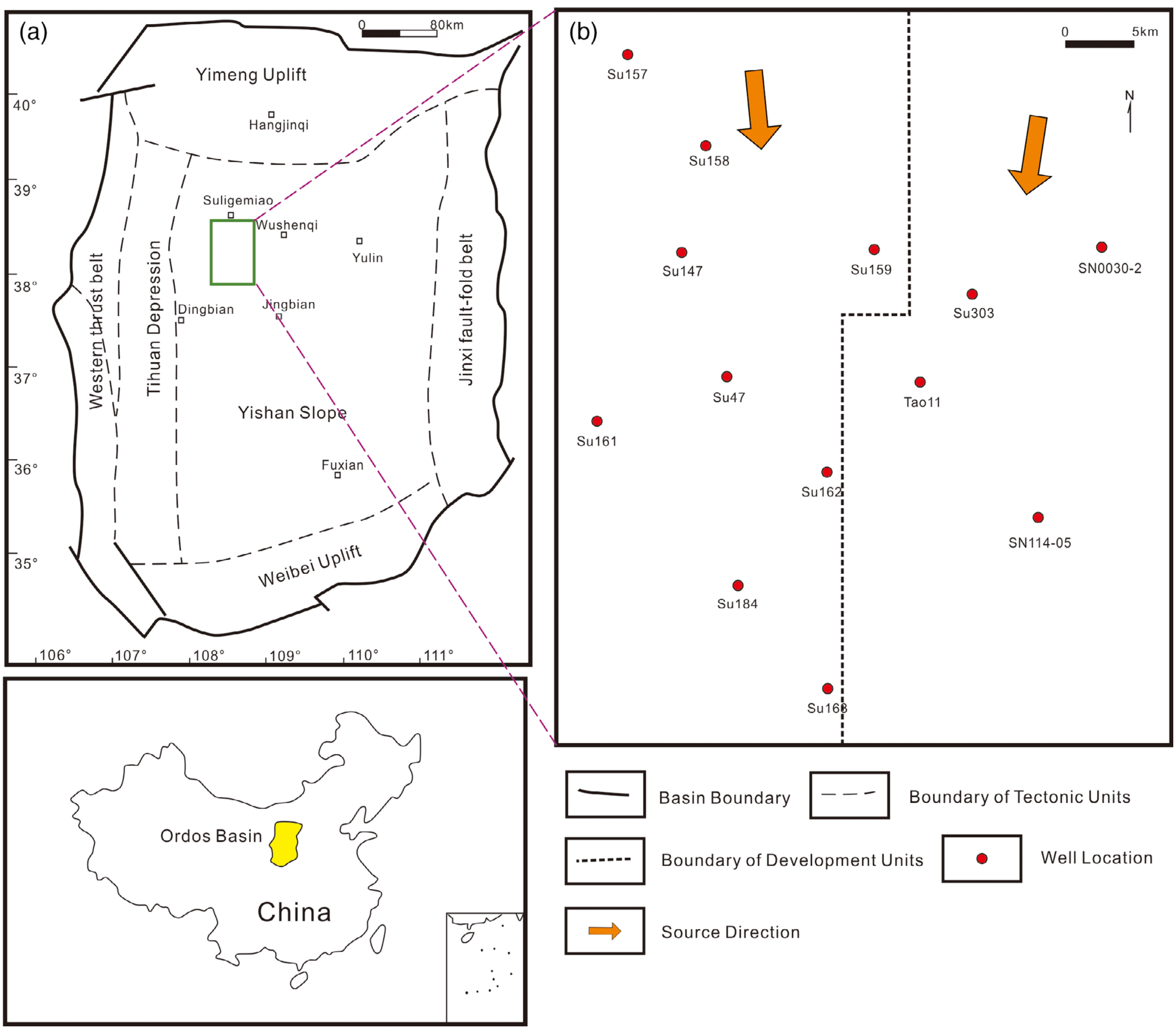

FIGURE 1 (a) Location of Sulige gas field and tectonic units in the Ordos Basin; (b) Well locations and sediment source direction of the study area [Colour figure can be viewed at wileyonlinelibrary.com]

studies have discussed about the depositional facies, diagenetic alterations, pore evolution, and factors control on reservoir quality in the Sulige area (Bao, Yang, Wang, & Nan, 2007; Bi et al., 2015; Chen, Hou, & Zhang, 2015; Fan, Wu, Wang, Zhang, & Guo, 2016; Liu & Sun, 2002; Yang, Fu, Liu, & Fan, 2012; Zhu, Liu, Zhong, & Han, 2009). However, little attention has been paid on how petrographic characteristics control reservoir quality of tight sandstones in coal-bearing strata of Sulige gas fields.

Therefore, the purposes of this paper are mainly focused on: (1) describing the sandstone composition and texture, (2) identifying

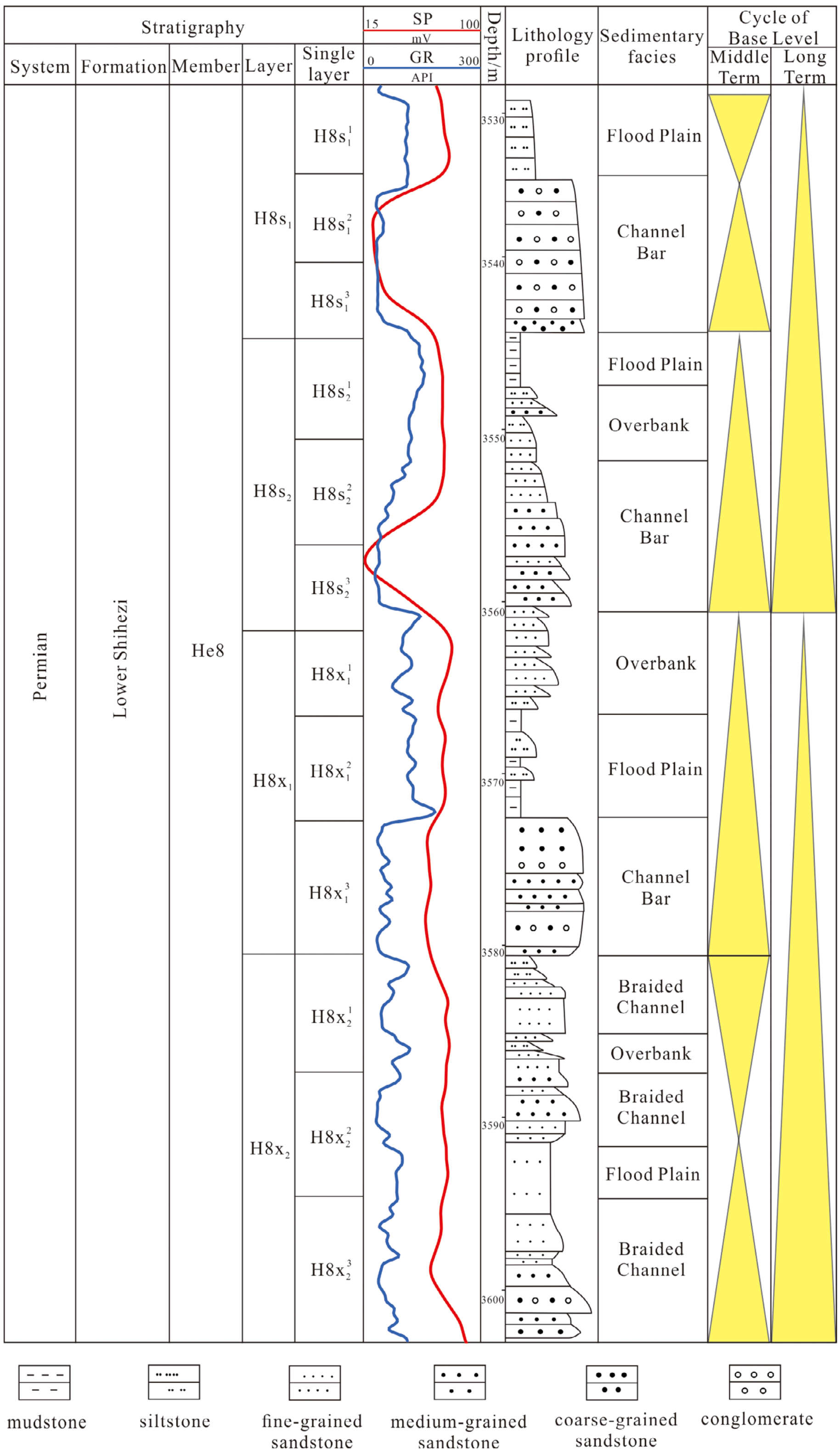

FIGURE 2 Detailed sequence stratigraphy and lithology section of He8 member in Ordos Basin (modified from Wang et al., 2011) [Colour figure can be viewed at wileyonlinelibrary.com]

TABLE 1 Petrographic characteristics and measured porosity-permeability values for some samples in Sulige area

Well name	Depth / m	Quartz / %	Chert / %	Feldspar / %	Rock fragments / %			Mica / %	Quartz cement / %	Calcite cement / %	Chlorite cement / %	Grain size / mm	Sorting	Φ / %	K / mD
					igneous	metamorphic	sedimentary								
Su303	3,563.12	55	1	0	3.5	20	0	2	1	0.5	5	0.4	Well	10.7	0.22
Su303	3,558.21	53	2	0	4	17	0	1	0	0	6	0.47	Well	11.47	0.27
Su303	3,560.06	61	2	0	3	14	0	1	0.5	2	5	0.45	Medium	12.17	0.63
Su303	3,556.89	55	1	0	4	17	0	2	0	0	0	0.37	Well	9.34	0.25
Su303	3,553.77	61	0.5	0	2	8.5	0	0	4	0	0	0.4	Well	12.56	0.2
Su303	3,566.02	66	0.5	0	2.5	6	0	1	0	0	0	0.42	Well	9.44	0.59
Su184	3,621.32	84.5	0.5	0	1.5	3	0.5	0	12	0	0.5	0.8	Well	9.7	1.22
Su163	3,613.09	82	2	2	0	5	2	1	3	2	0	0.48	Medium	5.77	0.24
Su163	3,610.2	80	2	3	0	4	9	1	3	0	0	0.18	Well	2.1	0.02
Su162	3,606.85	81	0	0	1.5	5.5	0	0	10	0	0	0.8	Well	4.75	0.21
Su162	3,605.67	78	3	0	0	3	0	0	9	0	0	0.65	Medium	9.67	0.78
Su161	3,600.46	61	5	0	2	8	0	0	3	0	4	0.2	Medium	1.63	0.01
Su158	3,597	70	2	0	3	8	0	0	4	0	0	0.5	Well	7.16	0.13
Su158	3,596	74	1	0	2	5	0	1	3	0	1	0.45	Medium	5.4	0.06
Su147	3,555.5	72	1	0	4	6	0	0.5	0	0	8	0.85	Well	12.66	0.78
SN114-05	3,547.8	21	4	0	1	51	5	1	6	0	0.5	0.33	Medium	6.98	0.34
SN114-05	3,547.49	37	4	0	1	40	2	0	6	0	0.5	0.4	Medium	6.88	0.35
SN114-05	3,566.55	56	5	0.25	0.5	19	2	1	1.5	2	0	0.23	Medium	2.4	0.04
SN114-05	3,569.71	50	6	0	1	22	4	2	3	0	0	0.25	Well	4.64	0.26

Note: Φ, measured porosity; K, measured permeability.

the source of various diagenetic minerals; (3) dividing sandstone types according to various petrographic characteristics, describing different diagenetic processes and reveal the controlling effect of petrophysics characteristics on them; (4) discussing the diagenetic evolution process and their coupling relationships with porosity evolution; and (5) unravelling how the process impacts the reservoir quality of tight reservoirs in coal-bearing strata of the four types of sandstones. The results can shed light on the formation mechanism and controlling factors of tight sandstones, which is useful for high-quality reservoir prediction in tight sandstone reservoirs.

2 | GEOLOGICAL SETTINGS

2.1 | Tectonic evolution and stratigraphy

The Ordos Basin is a multicycle craton located in western China which covers an area of 25×10^4 km^2 (Carroll, Graham, & Smith, 2010). It was filled with more than 10,000 m thickness of sediments (Carroll et al., 2010; Zhu et al., 2009). Six primary tectonic units were identified within the basin, namely, Yimeng Uplift, Thrust Belt, West Marginal Foreland, Tianhuan Depression, Jinxi Fault-fold Belt, Yishan Slope, and Weibei Uplift (Figure 1a) (Yang, Fan, Han, & Wang, 2012; Yang, Jin, Van Loon, Han, & Fan, 2017; Yang & Liu, 2014). The eastern part of the basin was rapidly uplifted and formed the westward-dipping monocline due to the Yanshan movement. There are few faults and folds developed in Yishan Slope, which is the main tectonic unit (Zhao, Zhang, Li, Cao, & Fan, 2014; Zhu et al., 2009). During the Caledonian movement in late Early Palaeozoic, the North China Block was uplifted, and erosion widely developed across the basin, thus leading to the loss of strata from Upper Ordovician to Lower Carboniferous (Li, Zhao, Yang, Fan, & Li, 2010; Yang et al., 2017). The upper Carboniferous strata contain Benxi Formation, while the Permian strata in the North China Block is represented by the Taiyuan Formation (P_1t), Shanxi Formation (P_2s), Shihezi Formation (P_2h), and Shiqianfeng Formation (P_3q) (Wang et al., 2011; Zhao et al., 2014).

The Sulige gas field is situated in the northwest of Yishan Slope, with few faults developed (Fan et al., 2019). The target layer is the Lower Shihezi Formation, which is 220–280 m in thickness and the He8 member (also the main reservoir) is 90–120 m thick, divided into four layers and 12 single layers (Figure 2). Meanwhile, the main gas-producing coal layers in the Shanxi and Taiyuan formations, have a thickness of 80–90 m and 25–30 m, respectively (Zhao et al., 2014).

2.2 | Depositional facies

The depositional facies of He8 member in the Ordos Basin have been well documented in many researches (Fic & Pedersen, 2013; Guo, Jia, He, Tang, & Liu, 2016; Li et al., 2010; Yang, Fu, Wei, & Liu, 2008; Yang & Liu, 2014). It is documented that the depositional environments of the He8 member in Sulige area are recognized as braided river (Guo et al., 2016). The facies can be characterized as braided channel, channel bar, flood plain, and overbank. The coal layers are widespread in flood plain in the Shanxi Formation, of which the main types are coking coal and gas coal, with a Ro value of 0.6% ~ 1% (Nie et al., 2017).

Provenance analysis shows that there are mixed sources in the study area from northeast and western area of the Hangjin Banner (Li et al., 2010; Xi, Wang, & Qin, 2002) (Figure 1b). The basement rocks in the northeast area mainly includes Archean chromite, granite, and purple granulite with a low quartz content (about 25%–60%). While the western area is dominated by meta-sedimentary rocks, containing reddish-white grey quartz, quartz sandstone, and dark-grey slate (Li et al., 2010). Quartz is the main component (volume 70–90%). Under the combined influence of source direction and sedimentary facies, the sedimentary composition and texture of He8 sandstones become very complicated.

3 | DATA AND METHODS

All the data are from 13 wells, including cores, conventional logging, and cutting samples. More than 200 samples covering different depositional facies in two source directions were chosen for analysis in order to get a credible conclusion. All experiment data about porosity and permeability, grain size, petrophysical property, XRD, and SEM were provided by Petro China Sulige gas field research center, Changqing Oilfield.

Porosity and permeability were measured from YRD-FKS-2 instrument after the samples were cut to 25× 50 mm columnar ones (Table 1). In order to determine the components as well as pore structure, more than 300 thin sections were used for point counts. All sections were impregnated with blue-dyed resin and a solution of Alizarin Red-S and potassium ferricyanide to highlight pores and carbonate minerals.

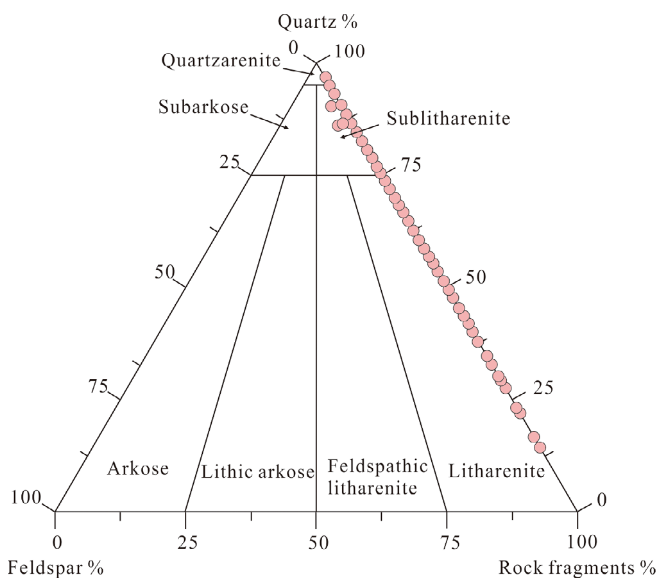

FIGURE 3 Triangular diagram of rock composition in He8 member sandstones [Colour figure can be viewed at wileyonlinelibrary.com]

Scanning electron microscope (SEM) and cathodoluminescence (CL) were both used to identify pore structure and different diagenetic minerals together with their characteristics and relative timing. A JEOL JSM-T330 scanning electron microscope was used for SEM analysis with 80 samples covered by a layer of gold. While 60 sections were applied for CL analysis with a Technosyn cold

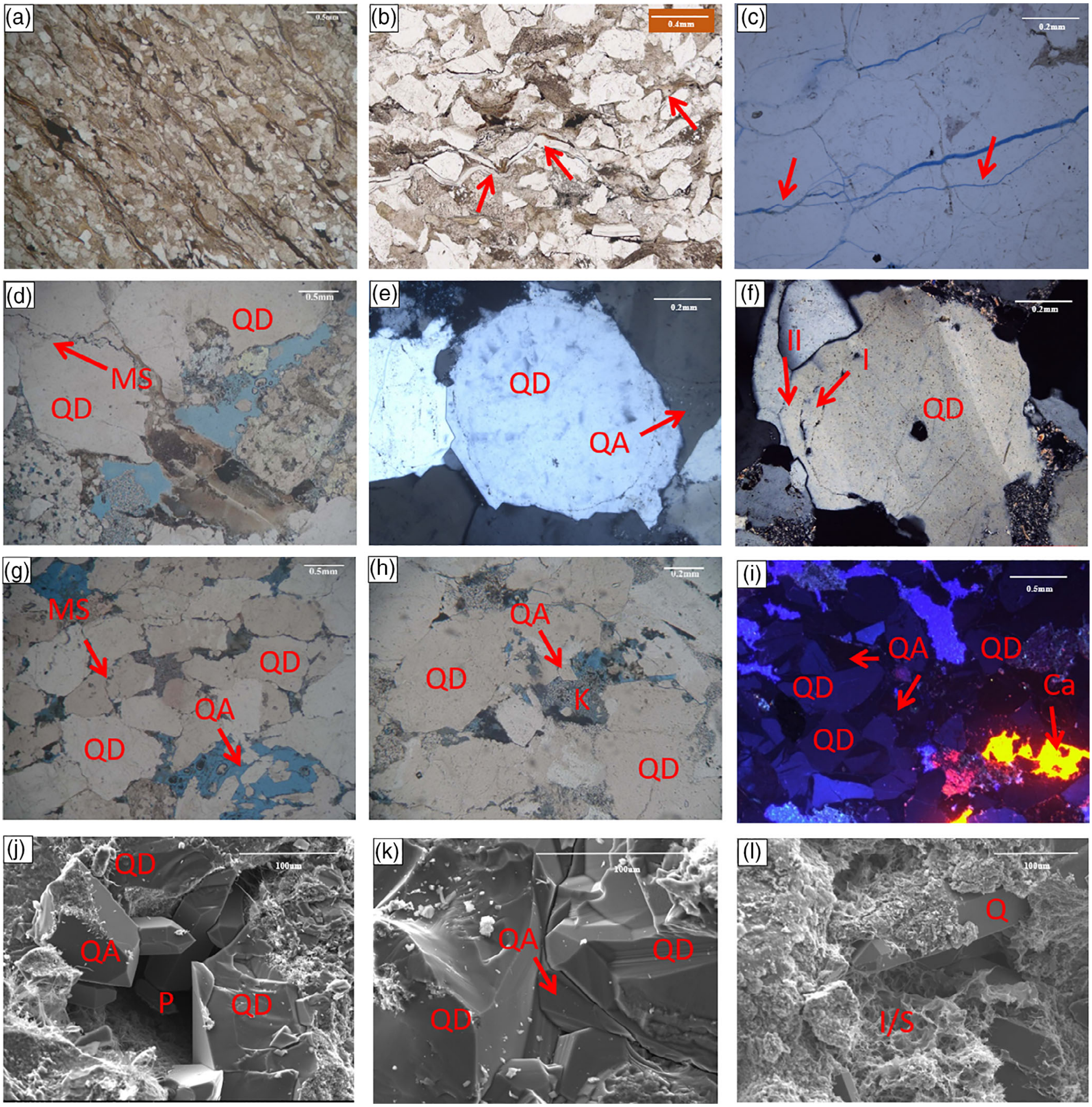

FIGURE 4 Compaction and quartz cement characteristics in He8 sandstone reservoir. (a) Compaction in fine-grained sandstone, well SN0030-2, 3,539.47 m; (b) Deformation of ductile grains, well SN0030-2, 3,728.02 m; (c) Fracture of detrital quartz, well Su147, 3,573.74 m; (d) Microscopic stylolites between detrital quartz, well SN114-05, 3,547.8 m; (e) Quartz overgrowth, well Su147, 3,573.74 m; (f) Two phases of quartz overgrowth (I and II), well Su147, 3,584.84 m; (g) Microscopic stylolites and quartz authigene in secondary pores, well SN114-05, 3,548.44 m; (h) Quartz authigene with kaolinite in secondary pores, well SN114-05, 3,544.38 m; (i) CL micrograph image show detrital quartz and quartz overgrowth, well Su147, 3,584.84 m; (j) SEM image show authigenic quartz filling in pores, well Su157, 3,609.15 m, (k) SEM image show quartz overgrowth around detrital quartz, well Su157, 3,617.52 m; (l) I/S mixed layers and authigenic quartz, well SN0030-2, 3,705.15 m. QD, detrital quartz grains; QA, authigenic quartz; P, pores; I/S, illite /smectite mixed layers; MS, microscopic stylolites; Ca, calcium [Colour figure can be viewed at wileyonlinelibrary.com]

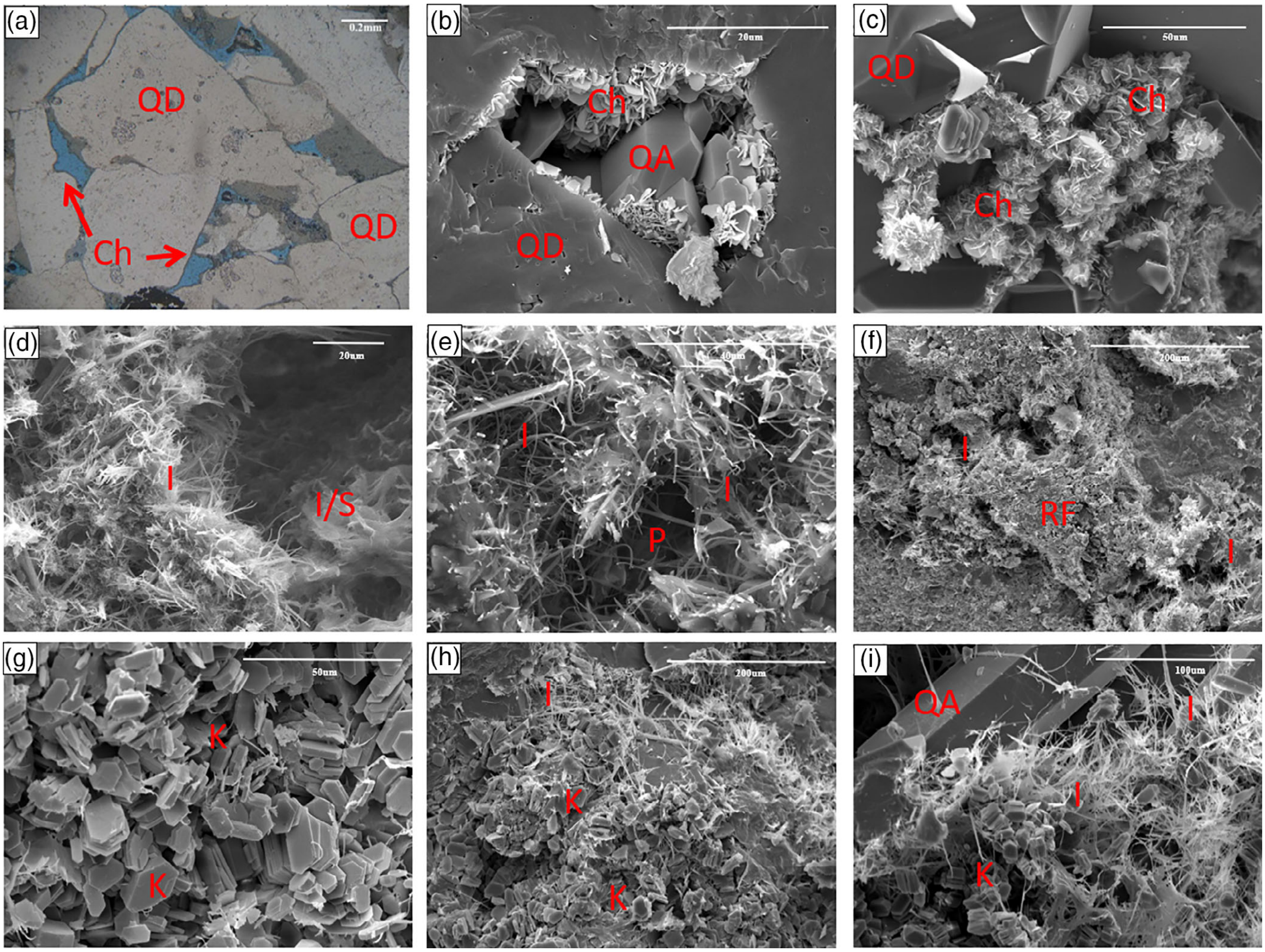

FIGURE 5 The characteristics of clay minerals in He8 sandstone reservoir. (a) Thin section image shows grain-coating chlorite around detrital quartz, well SN114-05, 3,531.1 m; (b) SEM image shows grain-coating chlorite and authigenic quartz, well SN114-05, 3,542.79 m; (c) Authigenic chlorite filling in pores, well Su47, 3,590.8 m; (d) Mixed-layer of illite/smectite and illite, well SN0030-2, 3,681.51 m; (e) Illite filling in pores, well Su47, 3,617.52 m; (f) Illitization of rock fragments, well SN114-05, 3,611.5 m; (g) SEM photo shows kaolinite, well SN114-05, 3,620.5 m; (h) SEM image shows illitization of kaolinite, well SN114-05, 3,555.92 m; (i) SEM image shows authigenic quartz along with kaolinite and illite, well SN114-05, 3,551.56 m. QD, detrital quartz grains; QA, authigenic quartz; P, pores; I/S, illite /smectite mixed layers; Ch, chlorite; K, kaolinite; I, illite [Colour figure can be viewed at wileyonlinelibrary.com]

cathodeluminoscope, of which the acceleration voltage was 0–20 kV with current of 200–400 mA.

X-ray diffraction (XRD) analysis was mainly used for determining species and volume of clay minerals as well as the ratio of I/S mixed layers. The fluid inclusions were measured on 25 samples through a LINKAM THMS-G600 heating-freezing stage. The rate of temperature change is 5°C/min and the temperatures were recorded when the bubbles disappeared.

4 | RESULTS

4.1 | Petrographic characteristics

Petrographic characteristics (sandstone composition, texture, etc.) play an important role in controlling diagenetic evolution (Lai et al., 2018; Morad et al., 2010). The main sandstones in He8 tight reservoirs are predominantly fine- to coarse-grained with moderate to well-sorting. Sandstones with different grain sizes can be identified as coarse-grained (over 0.5 mm) (commonly with conglomerate), medium-grained (0.25–0.5 mm), and fine-grained (0.1–0.25 mm). The main grain shapes vary from subangular to subrounded, with linear contacts and concavo-convex contacts among them. Furthermore, stylolites can also be found between grains indicating the tight compaction.

The analysis of petrology reveals that the detrital components comprise 14.00–84.5 0% quartz (average 60.97%), 0.00%–3.00% feldspars (average 0.05%), and 2.00–58% rock fragments (average 19.23%) (Table 1), showing that most of the sandstones are quartzarenite and sublitharenite with some litharenite, according to the classification scheme of Folk (1980) (Figure 3). Detrital quartz is the dominant grain in He8 sandstones, of which most are monocrystalline. Lithic fragments mainly comprise metamorphic fragments (include chert, quartzite, schistose, average 14.9%), volcanic fragments (mainly igneous, average 1.01%), sedimentary fragments (including shale and sandstone, average 1.18%), and mica (average 0.89%). Of these lithic fragments, large amounts of ductile fragments can be identified in He8 sandstones comprising volcanic fragments, mudstone fragments, and some metamorphic clasts. Based on data of thin section analysis, ductile fragments account for 0 to 26% (average 5.1%) of the volume of He8 sandstones.

According to varied petrographic characteristics (mainly grain size and detrital composition), six types of sandstone reservoirs can be distinguished, including: fine-grained litharenite, fine-grained quartzarenite, medium-grained litharenite, medium-grained quartzarenite, coarse-grained litharenite, and coarse-grained quartzarenite. Meanwhile, considering the important role that volcanic fragments play on reservoir quality (Zhu et al., 2009), each type of sandstone reservoir can be divided into two types: sandstones with abundant volcanic fragments (over 3%) and sandstones with few volcanic fragments (lower than 3%), resulting in a total of 12 types of sandstone reservoirs.

4.2 | Diagenetic mineralogy

Compaction, feldspar dissolution, quartz cementation, and clay transformations are important diagenetic events in He8 sandstones, leading to primary pores loss and plenty of diagenetic mineralogy.

4.2.1 | Quartz cement

The studies in thin section, SEM, and cathodoluminescence (CL) of He8 tight sandstones reveal that authigenic quartz is one of the main cements. It values range between 0.00 and 24.75% with an average of 5.35% (Figure 4a–f). Two kinds of quartz cementation modes, including quartz

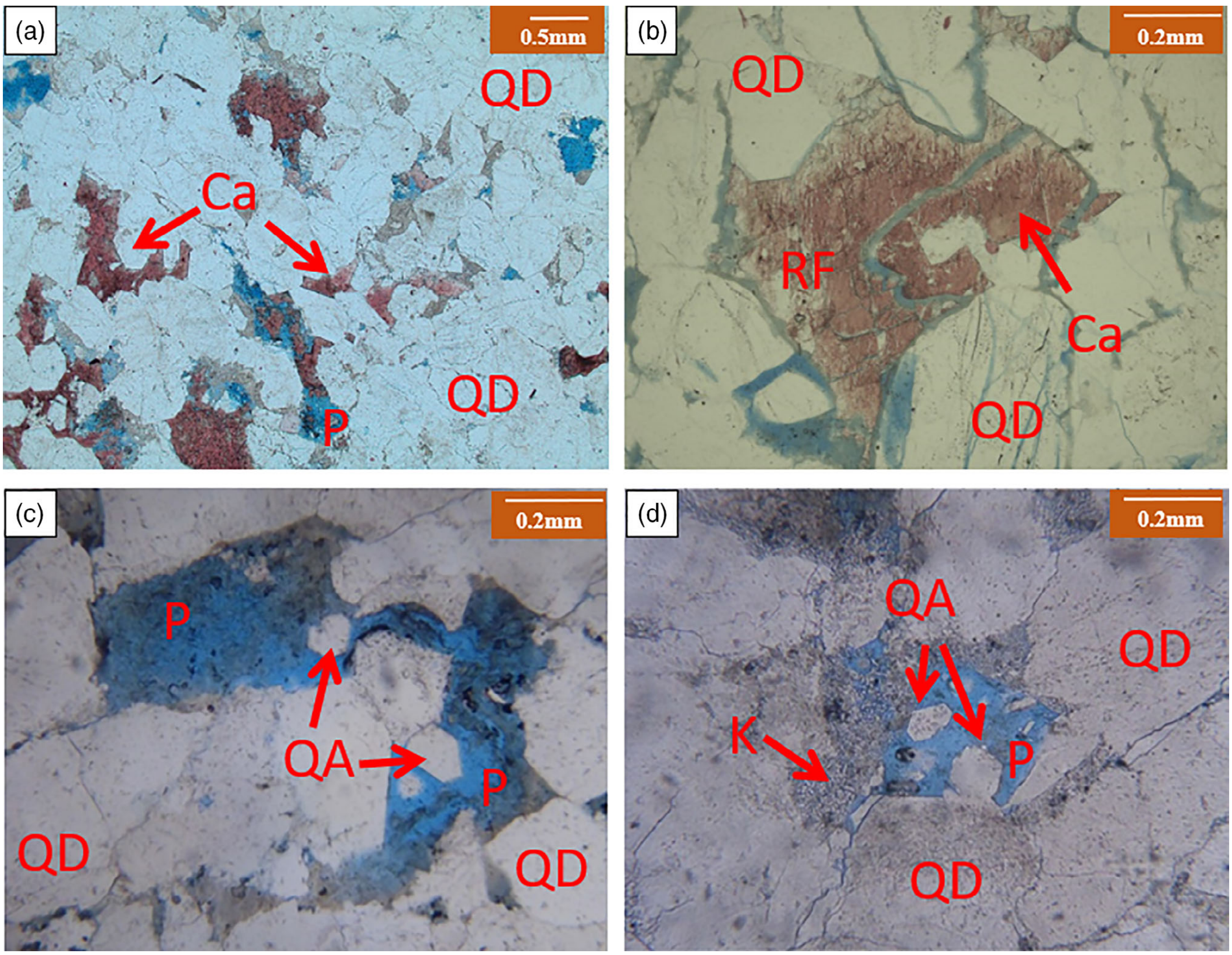

FIGURE 6 Photomicrographs showing calcite cement and K-feldspar dissolution pores. (a) Calcite filling in pores in tightly packed sandstones, well Su147, 3,784.84 m; (b) Calcite replaced rock fragment, well Su147, 3,573.74 m; (c) Dissolution pores of K-feldspar with authigenic quartz filling, well SN114-05, 3,572.34 m; (d) Dissolution pores of K-feldspar with authigenic quartz and kaolinite filling, well SN114-05, 3,567.9 m. QD, detrital quartz grains; QA, authigenic quartz; P, pores; K, kaolinite; Ca, calcium;RF, rock fragments [Colour figure can be viewed at wileyonlinelibrary.com]

overgrowth (Figure 4e,f), and pore-filling authigenic quartz (Figure 4g,h), can be discerned with the help of the microscope, CL, and SEM identification. The dust rims indicate quartz overgrowth from the detrital grains clearly under the microscope. Moreover, pore-filling authigenic quartz can be recognized by using CL and SEM study. For example, the boundaries are always shown clearly in CL images due to the brightly luminescent detrital grain and the darkly non-luminescent authigenic quartz (Figure 4i). The pore-filling quartz cements always occlude the primary pores and lead to significant reduction of the porosity. The diameters of the aggregates are between 30–100 μm as shown in Figure 4j. Furthermore, authigenic quartz is often accompanied with some clay minerals, such as illite, kaolinite, and chlorite (Figure 4l), while few quartz overgrowths exist where coated chlorite is present (Figure 5a,b).

4.2.2 | Clay minerals

The value of the total clay content, which ranges between 2 and 3%, with an average of 6.2%, is provided by XRD measurement. Also, four types of clay minerals are identified according to the XRD data, which include kaolinite (0 to 17.56%, average 2.87%), mixed-layer illite/smectite (trace to 4.45%, average 1.06%), chlorite (0 to 15.56%, average 2.25%), and illite (trace to 14%, average 5.27%). In addition, the mixed illite/smectite layers contain 75 to 90% illite, which are well-ordered.

Pore-filling and grain coating cements are two forms of chlorite cements. The pore-filling chlorites are always found in the pore space as a rose or flocculus habit (Figure 5c) when the grain coating chlorites usually grow close to and cover the grains (Figure 5a,b). The abundance of grain-coating chlorites plays a strong role in protecting primary pores from compaction (Ajdukiewicz & Lander, 2010; Lai, Wang, Ran, & Zhou, 2015; Nguyen et al., 2013). While, only 11 of 205 samples contain grain-coating chlorites, which explains why quartz cementations are generally developed in He8 sandstones.

As the thin section and SEM analysis showed, illite and I/S are found in two forms: (1) pore-filling cement and (2) grain replacement. Mixed layer of I/S occurs as honeycomb, while flaky and pore-filling illite show fibrous or flaky crystal in primary pores and in secondary pores blocking pore throats or bridging pores (Figure 5d,e). Illite forms as grain replacement are always observed as flaky or honeycombed morphology, accompanied with kaolinite and sometimes authigenic quartz (Figure 5f).

Kaolinite often occurs as a replacement of rock fragments or feldspars showing disordered booklets or vermicular aggregates (Figure 5g). Generally, kaolinite always exists together with fibrous illite within intergranular pores and minor amounts of microcrystalline authigenic quartz sometimes (Figure 5g–i).

4.2.3 | Carbonate cement

The routinely observed carbonate is a kind of minor component in He8 sandstone reservoirs, whose dominant cements are calcite and ferro-calcite. The calcite and ferro-calcite cements, which range from

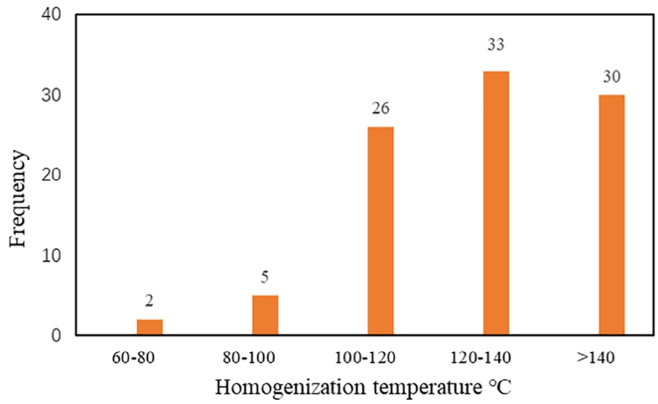

FIGURE 8 Homogenization temperature distribution of aqueous inclusions in quartz cements in He8 sandstone reservoirs [Colour figure can be viewed at wileyonlinelibrary.com]

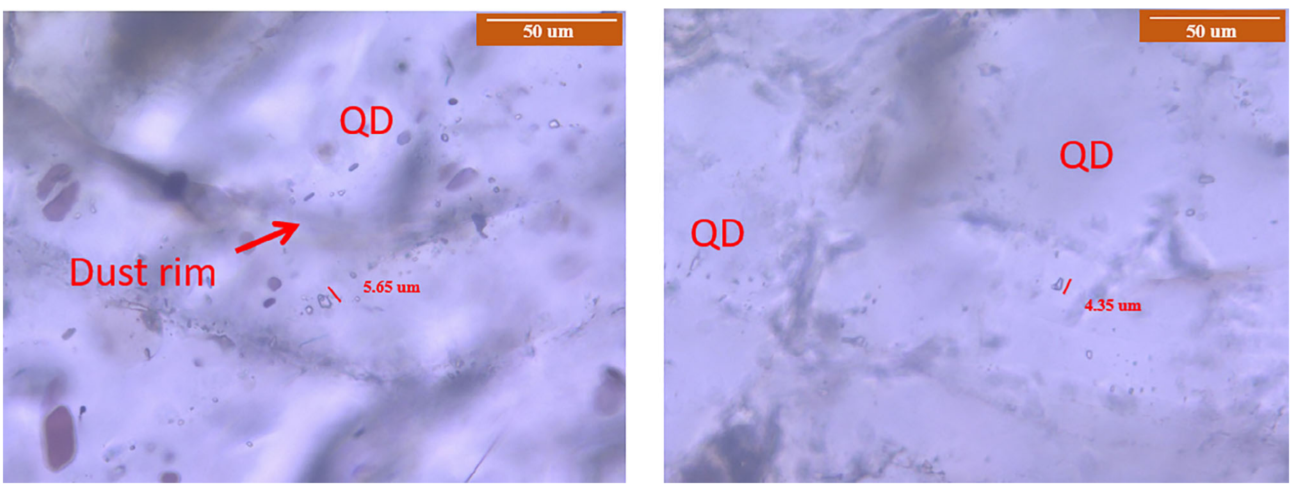

FIGURE 7 Characteristics of aqueous inclusions in quartz cements in He8 sandstones. QD, detrital quartz grains [Colour figure can be viewed at wileyonlinelibrary.com]

trace amounts to 11% and from 0 to 18%, respectively, have mean values of 1.89 and 0.86%. Calcite usually displays microcrystalline or coarsely crystalline habit when they fill the intergranular pores. It resulted in the propensity destruction (Figure 6a). Also, some calcite and ferro-calcite cements will replace framework grains such as rock fragments (Figure 6b). Late-diagenetic carbonate cements are clearly on CL images characterized by bright orange luminescence (Figure 5i), where early-diagenetic carbonate is absent due to the acid flow produced by coals during eodiagenesis.

4.2.4 | Feldspars

Through microscopic analysis, it is obvious that feldspars in He8 sandstones experienced strong dissolution and alteration. Few feldspars can be seen in thin section, CL and SEM, but some remaining pores due to feldspar dissolution, which have been recognized in many studies (Fan et al., 2016, 2019; Liu, Wu, Wei, Xiao, & Zhang, 2017). Plenty of kaolinite and authigenic quartz can been observed in dissolution pores of K-feldspars (Figure 6c,d).

4.3 | Fluid inclusions

The temperature of mineral precipitation can be predicted by the information from the aqueous inclusions (Robinson & Gluyas, 1992; Walderhaug, 1994). There are many aqueous inclusions in quartz overgrowths (Figure 7). The corresponding diameters range from 3.45 to 9.25 μm. At room temperature, most aqueous inclusions are two phases with gas bubbles. We found in total 96 aqueous inclusions located in the quartz overgrowths and pore-filling authigenic quartz and measured the homogenization temperatures (Th) (Figure 8). They range from about 70 to 155°C, and mainly centre on the range of 100–140°C, suggesting continuous quartz cementation process.

4.4 | Porosity and permeability

According to core plug analysis, the porosities of He8 sandstones range from 1.63 to 16.38% (average 7.02%) and the corresponding horizon permeabilities vary from 0.002 to 7.78 mD (average 0.36 mD). The range of porosity and permeability of different types of sandstones are quite different, as it is shown in the histogram (Figure 9).

It is obvious that some types of sandstones have similar reservoir quality. Putting them together, four categories can be observed: (1) fine-grained sandstones (Type I), including fine-grained quartzarenite and litharenite, whatever the content of volcanic fragments

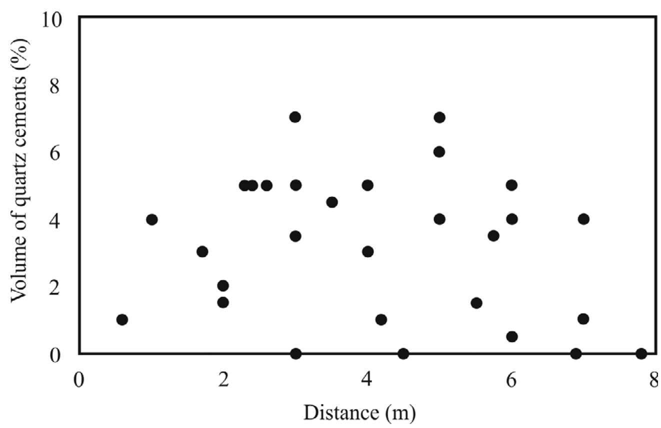

FIGURE 10 Plot show the volume of quartz cement versus the distance to contact surface between sandstones and muds

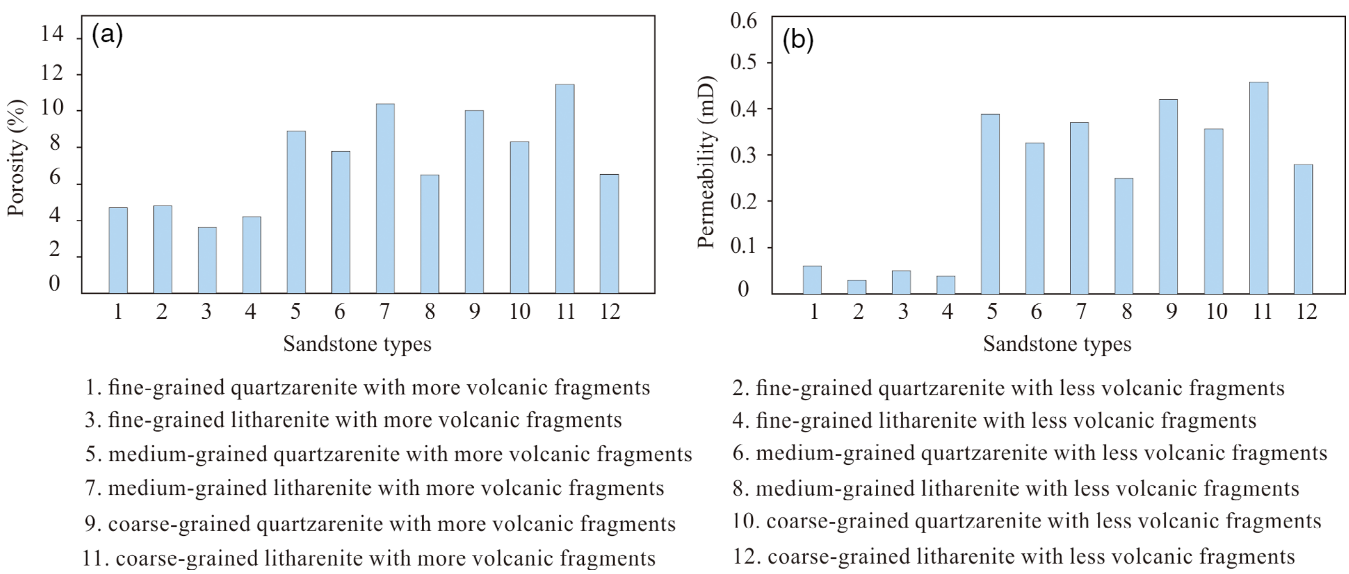

FIGURE 9 Histogram of (a) porosity and (b) permeability of different types of tight sandstones [Colour figure can be viewed at wileyonlinelibrary.com]

is; (2) medium- to coarse-grained sandstones with abundant volcanic fragments (Type II), including medium- to coarse-grained quartzarenite and litharenite with high amounts of volcanic fragments; (3) medium- to coarse-grained quartzarenite (Type III), including medium- to coarse-grained quartzarenite with low content of volcanic fragments; and (4) medium- to coarse-grained litharenite (Type IV), including medium- to coarse-grained litharenite with low content of volcanic fragments. As the main characteristics shown in Table 2, type II sandstones have the highest porosity and permeability (average 11% and 0.42 mD), followed by type III and type IV sandstones (average 8.2% and 0.38 mD; average 7.2% and 0.33 mD). While type I sandstones show the lowest properties (average 5.4% and 0.07 mD).

Three different types of pores can be identified according to the petrographic microscopy and SEM analysis, which are (1) primary intergranular porosity, (2) secondary porosity, and (3) micro-porosity (especially in clay minerals). Dissolution of unstable components such as feldspar (K-feldspar and plagioclase) and rock fragments (volcanic fragments) results in the formation of secondary pores. Also, it is not easy to identify the secondary pores along the granular boundaries from the primary pores. Generally, microfractures are not common in the studied sandstones.

TABLE 2 Main characteristics of different types of tight sandstones

Lithofacies	Depositional facies	Petrographic characteristics	Typical diagenetic events	Porosity / %	Permeability / mD
Type I	Overbank, floodplain	fine-grained sandstones,	Tense mechanical compaction, weak dissolution	1.63 ~ 8.2, avg. 5.4	0.01 ~ 0.2, avg. 0.07
Type II	Channel bar	medium- to coarse-grained sandstones, high amounts of volcanic fragments.	Formation of grain-coating chlorite, few quartz cements, calcite cementation.	7.3 ~ 12.66, avg. 11	0.23 ~ 0.78, avg. 0.42
Type III	Braided channels in western part of research area	medium- to coarse-grained sandstones, detrital quartz over 50%, low amounts of volcanic fragments.	Large amounts of quartz cements, kaolinite cementation	5.9 ~ 11.7 avg. 8.2	0.07 ~ 1.5 avg. 0.38
Type IV	braided channels in eastern part of research area	medium- to coarse-grained sandstones, lithics over 25%, low amounts of volcanic fragments.	large amounts of illite cements, Calcite cementation, Stronger Dissolution	4.5 ~ 13 avg. 7.2	0.1 ~ 0.7 avg. 0.33

5 | DISCUSSION

5.1 | Sources of quartz cement

Many studies have revealed the source of quartz cementation in tight sandstone reservoirs (Fan et al., 2019; Xi et al., 2015). However, the origins of silica may be different in tight sandstones in coal-bearing strata. There are various ways to provide sources of quartz cementation in sandstones, which can be detailed as clay mineral diagenesis, volcanic rock fragments reactions, detrital quartz grains dissolution and biogenic silica (Bjørlykke & Egeberg, 1993; Worden & Morad, 2000; Xi, Cao, et al., 2015). However, external source of silica is not under consideration although present in open-system diagenesis. Due to the low solubility of SiO_2 and Al^{3+}, it is hard to explain the long-distance transfer of a large amount of SiO_2 in theory (Bjørlykke, 2011; Bjørlykke, Mo, & Palm, 1988; Xi, Cao, et al., 2015). Also, the volume of quartz cement does not show significant relationship with the distance to the contact surface between sandstones and muds, which indicates that quartz cement is independent from outside sources (Figure 10).

Biogenic silica dissolution such as siliceous sponge spicules is also a likely source of silica (Aase & Walderhaug, 2005; Xi, Cao, et al., 2015). However, there is no evidence showing biogenic silica materials exist either under the microscope or in previous studies. Thus, biogenic silica may not be a source of quartz cement in He8 sandstones.

Smectite transformation into illite through I/S mixed layers may produce silica for quartz cement with the increasing temperature in many research studies (Bjørlykke, 2011; Lynch, Mack, & Land, 1997; Xi, Cao, et al., 2015). In general, smectite is easily transformed from volcanic fragments during early diagenesis (Hodder, Naish, & Nelson, 1993; Lai, Wang, Ran, Zhou, & Cui, 2016; Shoval, 2004;

Wang & Mou, 2013; Yang, Yang, Shi, & Yin, 2007), which are abundant in He8 sandstones as described in the petrologic analysis. Then smectite would transform to order I/S mixed layers with enough potassium as the temperature increases (Bjørlykke, 2014). When the silicas are precipitated, the reaction will continue as:

$$1.5Al_2Si_4O_{10}(OH)_2(\text{Smectite}) + K^+ = KAl_3Si_3O_{10}(OH)_2(\text{Illite}) + 3SiO_2 + H^+ \quad (1)$$

It has been discussed that the transformation of smectite occurs at around 70°C and enough supply of K^+ is required for the reaction to proceed (Metwally & Chesnokov, 2012; Peltonen, Marcussen, & Jahren, 2009; Thyberg et al., 2010). In He8 sandstones, K-feldspar dissolution can be a source of potassium due to the commonly observed dissolution pores by electron microscopy (Figure 6c,d). However, reaction (1) can be limited because the dissolution of K-feldspars will not be much until the temperature is over 120°C (Nguyen et al., 2013; Yuan et al., 2015). What is more, the homogenization temperature distribution of inclusions in quartz overgrowth shows a similar result. Although the distribution starts from 60–80°C, which meets the temperature of reaction (1), only two of 96 study samples show a homogenization temperature between 60–80°C, indicating the source of silica produced by reaction (1) may not be the major source (Figure 8).

A possible source of quartz cement may also come from K-feldspar dissolution and transformation of volcanic rock fragments (Giles & De Boer, 1990; Xi, Cao, et al., 2015). Both can produce an amount of smectites which can be a source for quartz cementation. Dissolution of K-feldspars can be expressed by reaction (2):

$$\begin{aligned} &2KAlSi_3O_8(\text{K-feldspar}) + 2H^+ + H_2O \\ &= Al_2Si_2O_5(OH)_4(\text{Kaolinite}) + 4SiO_2 + 2K^+ \end{aligned} \quad (2)$$

Leaching by meteoric water during shallow open-system diagenesis may cause this reaction (Bjørlykke & Jahren, 2012). However, the dissolution of K-feldspars can be limited because of the increasing concentration of K^+ and stability of K-feldspars. When the depth increases and the temperature is over 120°C, the coal will release large amounts of organic acid and CO_2, resulting in an amount of dissolution of K-feldspars accompanied by quartz cementation. Some amounts of microcrystalline quartz observed in secondary pores formed by feldspar dissolution are good supporting evidence.

When the temperature reaches 130°C as the buried depth increases, kaolinite and K-feldspar will not coexist stably (Bjørlykke, 2014; Dutton & Loucks, 2010; Lanson et al., 2002; Srodon, 1999), and the reaction between them can be simplified as:

$$Al_2Si_2O_5(OH)_4(\text{Kaolinite}) + KAlSi_3O_8(\text{K-feldspar}) \rightarrow$$

$$KAlSi_3O_{10}(OH)_2(\text{Illite}) + 2SiO_2 + H_2O \quad (3)$$

In this process, K-feldspar reacts with kaolinite and produces illite and quartz. It is evident that the illite can replace the kaolinite accompanied by authigenic quartz (Figure 5h,i). What is more, the homogenization temperature above 130°C (Figure 8) and the negative correlation relationship of illite and kaolinite both reveal this reaction (Figure 11). Generally, all the K-feldspar have transformed either to kaolinite or illite for there is little K-feldspar that can be seen in thin section.

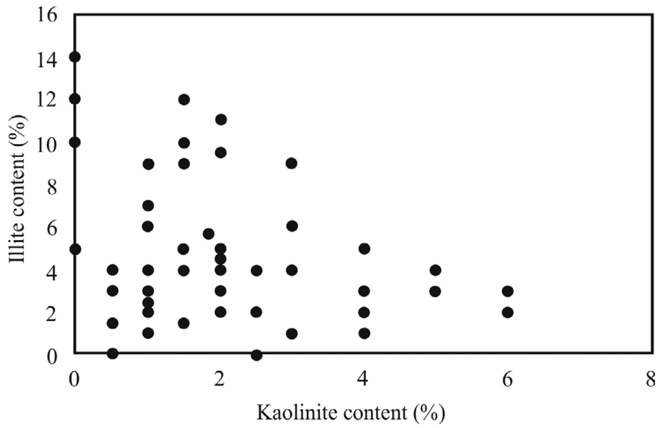

FIGURE 11 Plot showing kaolinite content versus illite content

The micro-stylolites commonly observed between detrital quartz grains indicate that pressure solution is also a main source of silica in He8 sandstones (Figure 4d,g). It has been discussed that pressure solution can be induced and promoted when there are rich clay minerals (Molenaar, Cyziene, & Sliaupa, 2007). Thus, it can provide plenty of silica due to the abundant clay minerals, as it is shown in the petrology. The silica forms at the contact surface of grains or along the micro-stylolites as a result of pressure solution. Then it spreads to the grain surfaces or pores and precipitates as quartz cementation (Bjørlykke & Jahren, 2012; Hyodo, Kozdon, Pollington, & Valley, 2014). Furthermore, silica produced by chemical compaction exists during the burial process, which is in accordance with the continuous distribution of the homogenization temperature.

5.2 | Petrographic characteristics control on diagenesis

Petrographic characteristics including grain size, sorting, and detrital composition have been proved having significant impact on diagenetic process, especially on compaction and cementation (Bjørlykke, 2014; Lai et al., 2016, 2017; Li et al., 2017). However, the impact of petrographic characteristics on diagenesis of tight sandstone reservoir in coal-bearing strata can be much different due to the feldspar dissolution caused by evolution of coal (Wang & Mou, 2013). The absence of feldspar enlarged the impact of other detrital compositions such as quartz and fragments on diagenesis. Furthermore, the different distribution of tuffaceous matrix also greatly affects the diagenetic alteration (Zhu et al., 2009).

Mechanical compaction is the main reason that made the He8 sandstones tight by losing porosity immediately after deposition (Figure 12). Meanwhile, grain size and detrital composition are factors

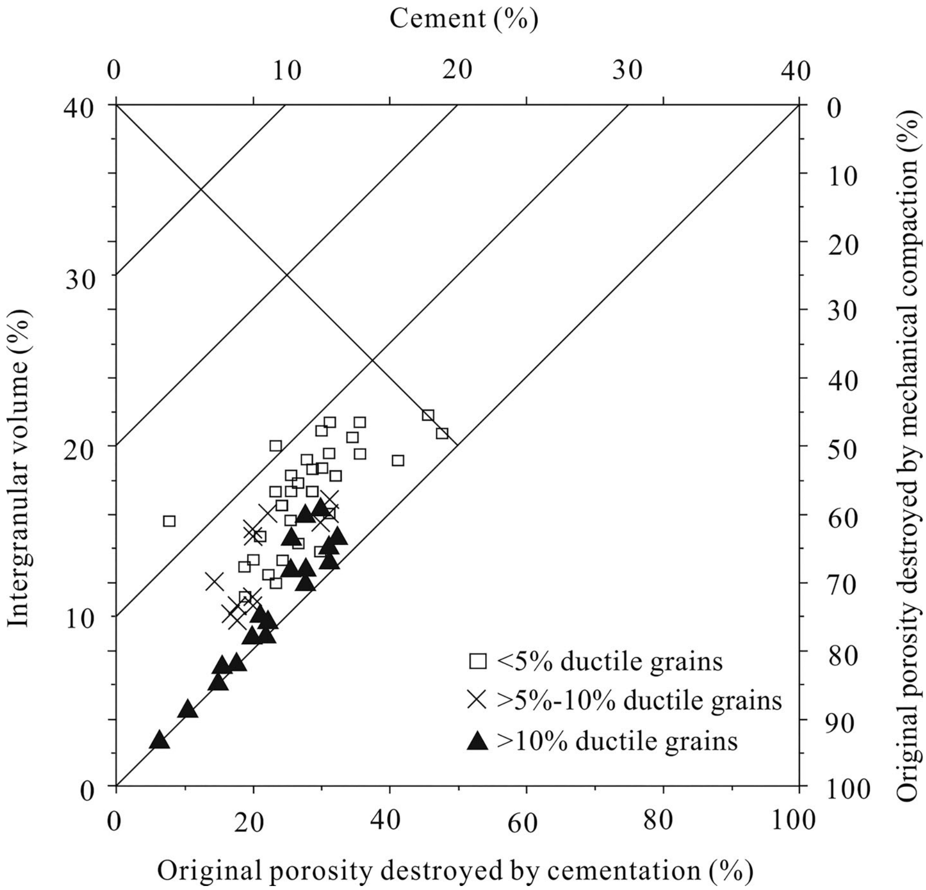

FIGURE 12 Content of cements versus intergranular volume (IGV)

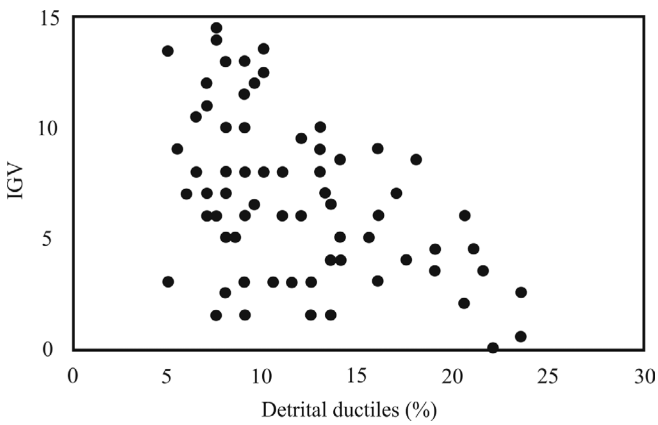

FIGURE 13 Intergranular volume (IGV) versus content of detrital ductiles

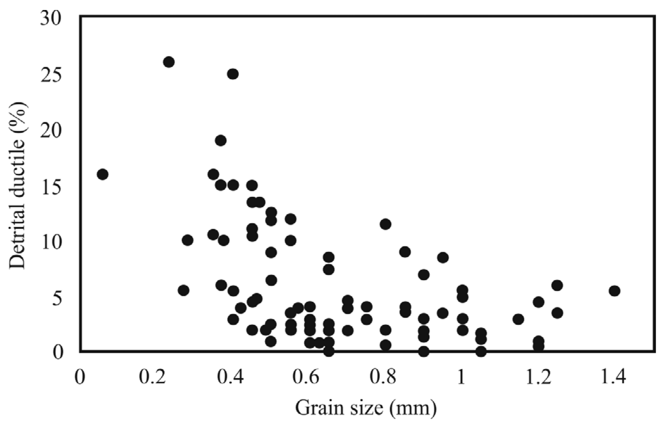

FIGURE 14 Content of detrital ductiles versus average detrital grain size

affecting mechanical compaction as the sandstones in He8 member are of moderately to well-sorted. Previous studies have showed that fine-grained sandstones may suffer dense compaction (Li et al., 2017). Also, large amounts of ductile grains, such as clays and certain volcanic rock fragments, may lead to a greater degree of compaction (Li, Guo, Li, & Wang, 2020; Rahman & Worden, 2016; Worden & Morad, 2000) (Figure 12). As is shown in Figure 13, IGV decreases with the increase of the content of ductile fragments. Moreover, there tend to be less ductile fragments in coarser grained sandstones while more in finer grained sandstones (Figure 14). Both can cause different levels of compaction in coarse- and fine-grained sandstones. In addition, the high degree of compaction is attributed to the lack of early cements. The amount of acidic fluid that flows into the reservoir in early diagenesis because of the organic matter of coal layers (Fan et al., 2019; Wang & Mou, 2013; Zhu et al., 2009), inhibits the formation of eogenetic calcium cements, thus resulting in greater compaction.

Quartz cementation is also influenced greatly by grain size and detrital composition in He8 tight sandstone reservoirs. Coarse-grained

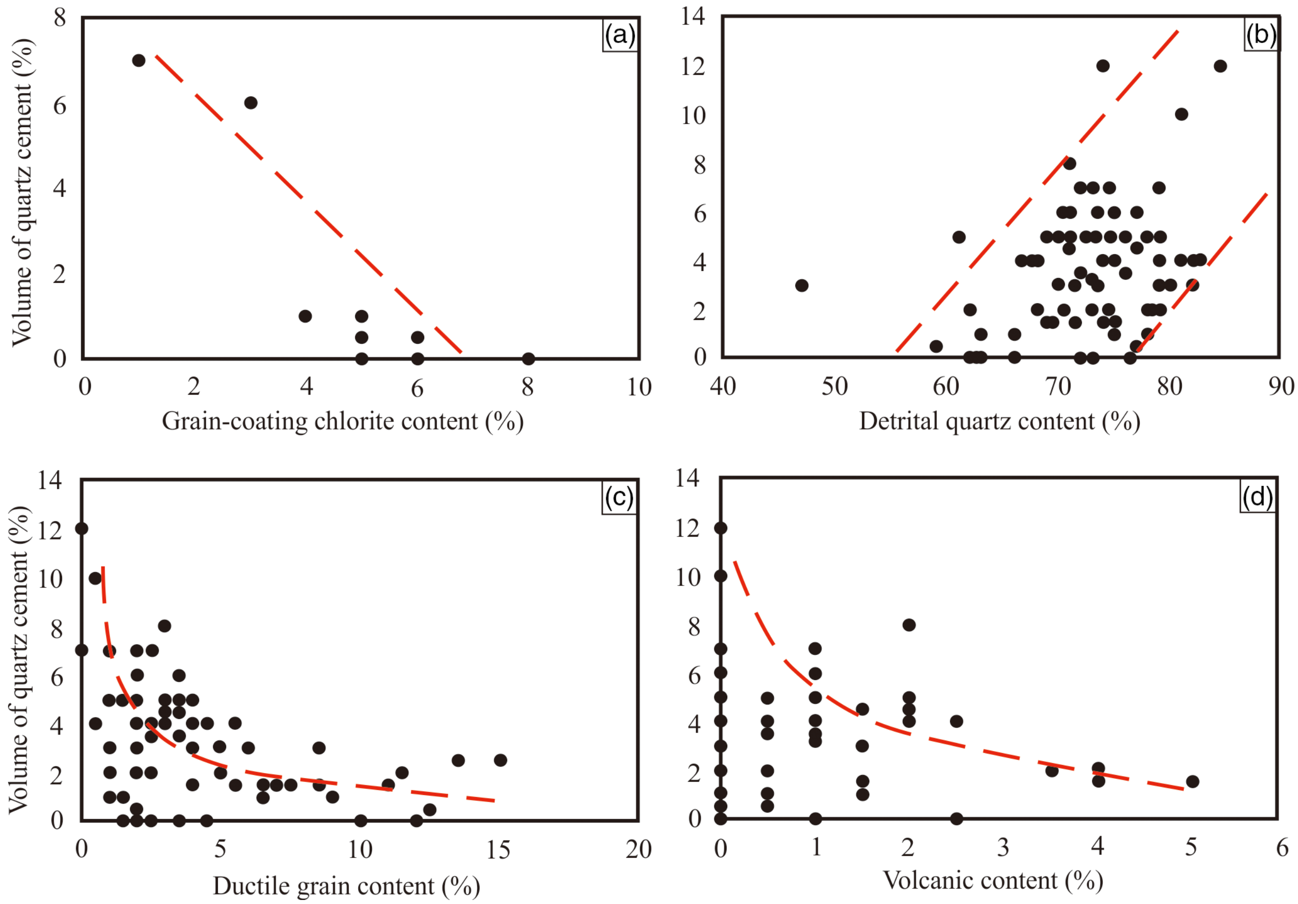

FIGURE 15 Relationship between (a) grain-coating chlorites, (b) detrital quartz content, (c) ductile grain content, (d) volcanic content and volume of quartz cements [Colour figure can be viewed at wileyonlinelibrary.com]

sandstones with abundant volcanic rock fragment and tuffaceous lithics would form grain-coating chlorite associating to the sufficient Fe^{2+} and Mg^{2+}, which were released by alteration of volcanics (Storvoll, Bjørlykke, Karlsen, & Saigal, 2002; Zhu et al., 2009). The presence of grain-coating chlorites is very important on inhibiting the formation of quartz overgrowth during burial, as has been explained in many researches (Ajdukiewicz & Lander, 2010). Well-developed grain-coating chlorite will cover the detrital quartz surface thus reducing the nucleation of siliceous grains (Ajdukiewicz & Lander, 2010; Ajdukiewicz & Larese, 2012; Heald & Renton, 1966; Lander, Larese, & Bonnell, 2008). Although grain-coating chlorites are not commonly found in He8 sandstones, there is still a negative correlation between the volume of chlorite coating and quartz overgrowth (Figure 15a).

The content of detrital quartz is also an important factor for sandstones with similar grain size according to Figure 15b. More detrital quartz means more contact areas between clastic grains. Thus, more silica is released due to microstylolites formed by chemical compaction. What is more, sufficient surface area in quartz-rich sandstones is beneficial to the nucleation of silica.

The amount of quartz cementation also shows a significant trend, with the amounts of ductile fragments (volcanic, mudstone, and some metamorphic) (Figure 15c). As discussed before, the volcanic rock fragments can provide some silica for quartz cementation by turning to smectite during eodiagenesis. If more volcanic rock fragments are preserved, the content of silica for quartz cementation will be insufficient, resulting in the negative correlation between quartz cementation content and volcanic content (Figure 15d). Furthermore, sandstones with remaining volcanic and other ductile fragments will experience more intense compaction, resulting in deformation of fragments or filling in pores as pseudomatrix. These deformed volcanic or ductile fragments contact tightly to detrital quartz and cover most of the surface area, thus reducing the nucleation of silica.

5.3 | Diagenetic phases and its evolution sequence

Due to complex thermal evolution of coal layers, diagenetic process could be much different in tight sandstone reservoirs in coal-bearing strata. According to the characteristics, distributions, and spatial relationships of different diagenetic minerals in thin section, CL, and SEM observations, a paragenetic sequence has been constructed. In general, the diagenetic process can be divided into three stages: eodiagenesis (commonly 0–2 km depth, <80°C and smectite content over 50% in the I/S), early meso-diagenesis (commonly 2–3 km depth, 80–130°C and smectite content 50 to 15% in the I/S), and late meso-diagenesis (commonly >3 km depth, >130°C and smectite content less than 15% in the I/S). However, it is impossible to accurately define the timing and duration of all diagenetic events as a result of the complicated burial history.

5.3.1 | Eodiagenesis

The types and degrees of diagenesis during eodiagenesis play a significant role in subsequent alterations and reservoir evolution (Li et al., 2020; Mansurbeg et al., 2008; Wang & Mou, 2013). The main diagenetic events are as follows: (1) mechanical compaction; (2) early dissolution of acid water and feldspar alteration to kaolinite; (3) chlorite coating around grains, and (4) cementation of quartz.

During the early stage of coal evolution, large amounts of acid was released leading to the dissolution of early calcite cements, which is much more than that in non-coal-bearing strata (Shuai et al., 2013; Zhen & Feng, 1997). Few early cements promoted the heavy compaction, leading to deformation of micas and ductile grains as well as fractures in rigid grains (Figure 4c). The frequently observed planar and concavo-convex grain contacts also show the results of pressure dissolution (Figure 4a,b). In other aspects, the acid fluids resulted in dissolution of feldspars and lithic fragments in He8 sandstone reservoirs. Plagioclase tended to dissolve first rather than K-feldspars because of its instabilities and pore-filling kaolinite usually precipitates where dissolution happened. Meanwhile, the presence of quartz cement is another result of feldspar dissolution. Chlorite usually formed on the clean detrital quartz with Fe^{2+} and Mg^{2+} after the alteration of

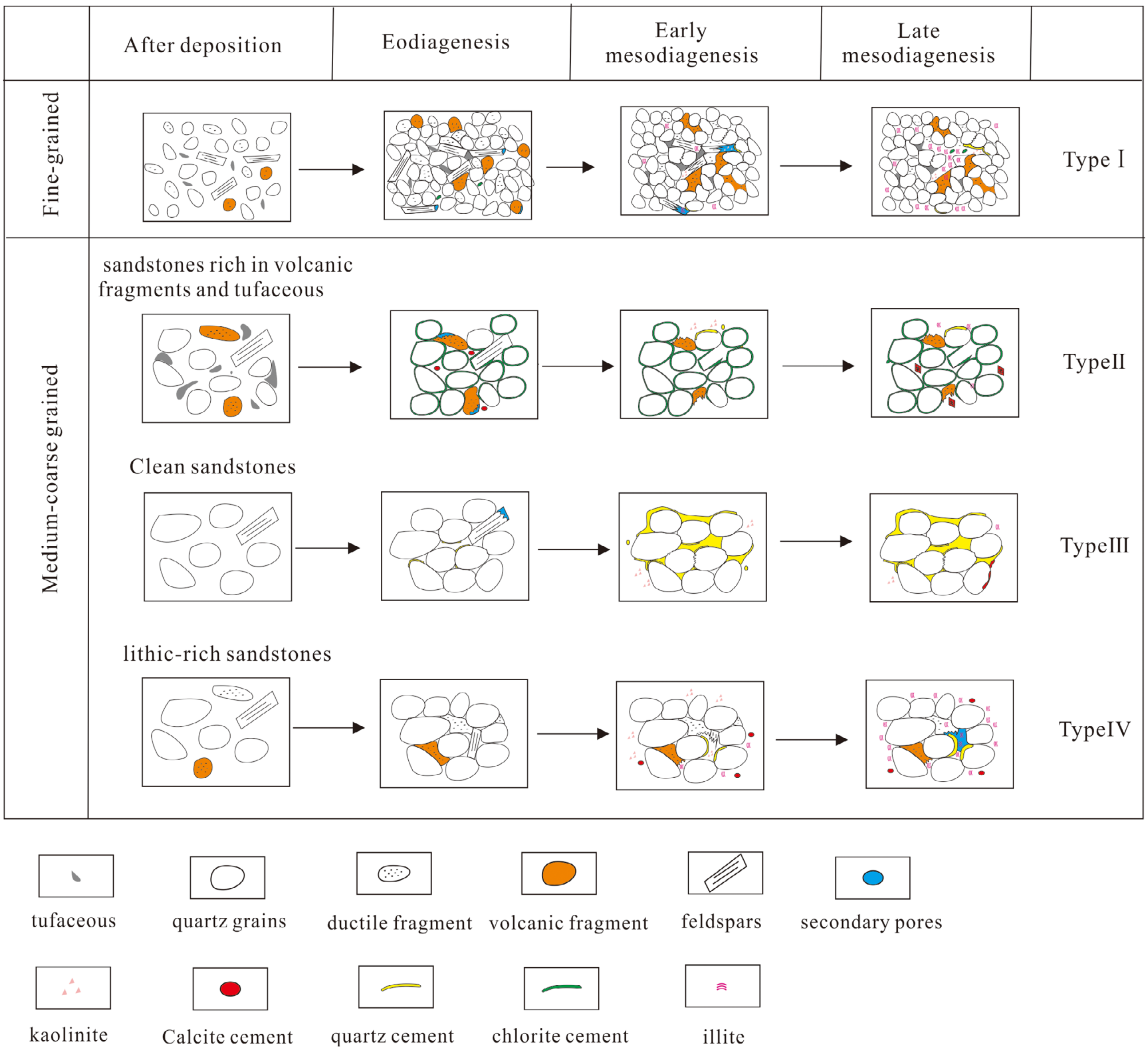

FIGURE 16 Diagenesis sequence of different types of sandstone reservoirs in Sulige gas field [Colour figure can be viewed at wileyonlinelibrary.com]

volcanic fragments and tuffaceous matrix (Zhu et al., 2009). Smectite was another product of the alteration of volcanic fragments, some of which transformed into honeycomb-like illite.

Among the four types of sandstones, type I sandstones suffered the tightest compaction due to the high ductile contents and the dissolution was limited because of the rapid loss of pores despite many instable fragments such as volcanic fragments. Chlorite coating in type II sandstone prevented it from dense compaction and quartz cement. Although more dissolution would happen in type III and type IV sandstones, diagenetic minerals such as quartz overgrowth and kaolinite were still very little. This is because of the limited dissolution of feldspar at a temperature under 80°C.

5.3.2 | Early meso-diagenesis

Diagenetic events in early meso-diagenesis mainly included (1) progressive burial and mechanical compaction, (2) large amounts of quartz cementation, and (3) dissolution of feldspars.

During early meso-diagenesis, mechanical compaction continued to increase and further reduce primary pores in He8 sandstones. When the burial depth and temperature increased, large amounts of organic acid and CO_2 will be released by coals during pyrolysis, resulting in the dissolution of feldspars and rock fragments. The dissolution produced large number of secondary pores, which can be frequently observed through microscopy as honeycomb porosity (Figure 5e). Feldspars can be altered into kaolinite and quartz, as shown in Reaction (1), especially when the temperature is over 120°C (Higgs, Zwingmann, Reyes, Funnell, & Higgs, 2007; Yuan et al., 2015), which is one of the main sources of quartz cements.

Among the four types of sandstones, type I sandstones continued suffering dense compaction, resulting in more loss of porosity. Type II sandstones underwent a weaker compaction as well as quartz cementation, thanks to the grain-coating chlorite. Quartz cementation in type II sandstones is mainly in the form of microquartz, rather than quartz overgrowth, with an average of 0.3% in intergranular pores. In contrast, there are large amounts of quartz overgrowth in type III sandstones, with an average of 4.5%, occupying most of the intergranular pores (Figure 16). Type IV sandstones preferred a lot of pseudomatrix formed by compaction, which limited large amounts of quartz overgrowth, as discussed in Section 5.2. Also, secondary pores in lithic fragments are also commonly observed, which contribute much to porosity in type IV sandstones.

5.3.3 | Late meso-diagenesis

When it comes to a great depth, the temperature was more than 130°C. The following diagenetic events were important: (1) the cementation of calcite and ferrous calcite, (2) the filling of chlorite, and (3) the formation of illite.

When the temperature was over 130°C, the organic matter became over-mature and the rate of organic acid production decreased. As a result, pore water changed from acid to weakly alkaline, which promoted the cementation by calcite and ferro-calcite. Ferro-calcite always exists when there are abundant volcanic fragments forming large amounts of remaining Fe^{2+} through dissolution. In deeply buried sandstones, kaolinite would transform to illite when it was over 130°C with enough potassium from K-feldspar dissolution as shown in reaction (2) (Bjørlykke, 2014). When there was enough Fe^{2+}, Mg^{2+}, kaolinite can also turn to chlorite (Wang & Mou, 2013), filling the secondary pores. Consequently, almost all illite-smectite mixed-layer had transformed to illite layers during late meso-diagenesis, leaving the clay minerals of He8 sandstones dominated by illite and chlorite, with kaolinite absent.

Among the four types of sandstones, type IV sandstones usually have the most calcite and ferro-calcite cementation (average 1.6%) due to sufficient space formed during dissolution, followed by type II sandstones (average 0.8%). As a comparison, type III sandstone contents only 0.6% calcite cementation on average for quartz overgrowth have occupied most space. What is more, illite is frequently observed in type IV sandstones, which formed from kaolinite produced during dissolution (Figure 16).

5.4 | Controls on reservoir quality

5.4.1 | Control of diagenesis on reservoir quality

Diagenetic events including compaction, cementation, and dissolution play an important role on reservoir quality (Kim, Lee, & Hisada, 2007; Walderhaug, 2000; Worden, Mayall, & Evans, 2000; Xi, Liu, & Meng, 2015; Yang, Fan, Van Loon, Han, & Wang, 2014). Mechanical compaction is the main reason for the low reservoir quality in He8 sandstones, where porosity reduced by compaction can be up to 15–38% according to porosity evolution analysis. Also, the plot of total intergranular volume versus total cements (Figure 12), estimating the original porosity ranging from 38 to 40% (Beard & Weyl, 1973), shows that more loss of primary porosity is caused by compaction but not cementation.

The impact of cements on the reservoir quality is complicated. Quartz cement will occupy the pores and lead to significant porosity and permeability reduction (Figure 17a). However, unlike the rapid decrease in other types of sandstones, the permeability of type III sandstones only decreases when the volume of quartz cementation is over 6% (Figure 17b). The reason is that the main form of quartz cement in type III sandstone is quartz overgrowth, which will first precipitate at the margin of the grains, thus having little effect on permeability. As it increased, the enlargement will contact and finally block the pores, resulting in low permeability.

Another important diagenetic mineral that affects much on the reservoir quality of He8 sandstones is chlorite. It is well known that grain-coating chlorites can prevent sandstones from quartz cementation and preserve primary pores, while the reservoir quality may also be poor, if the thickness of chlorite increases too much, thus filling pores and throats (Wang, Chang, et al., 2017). However, it shows a

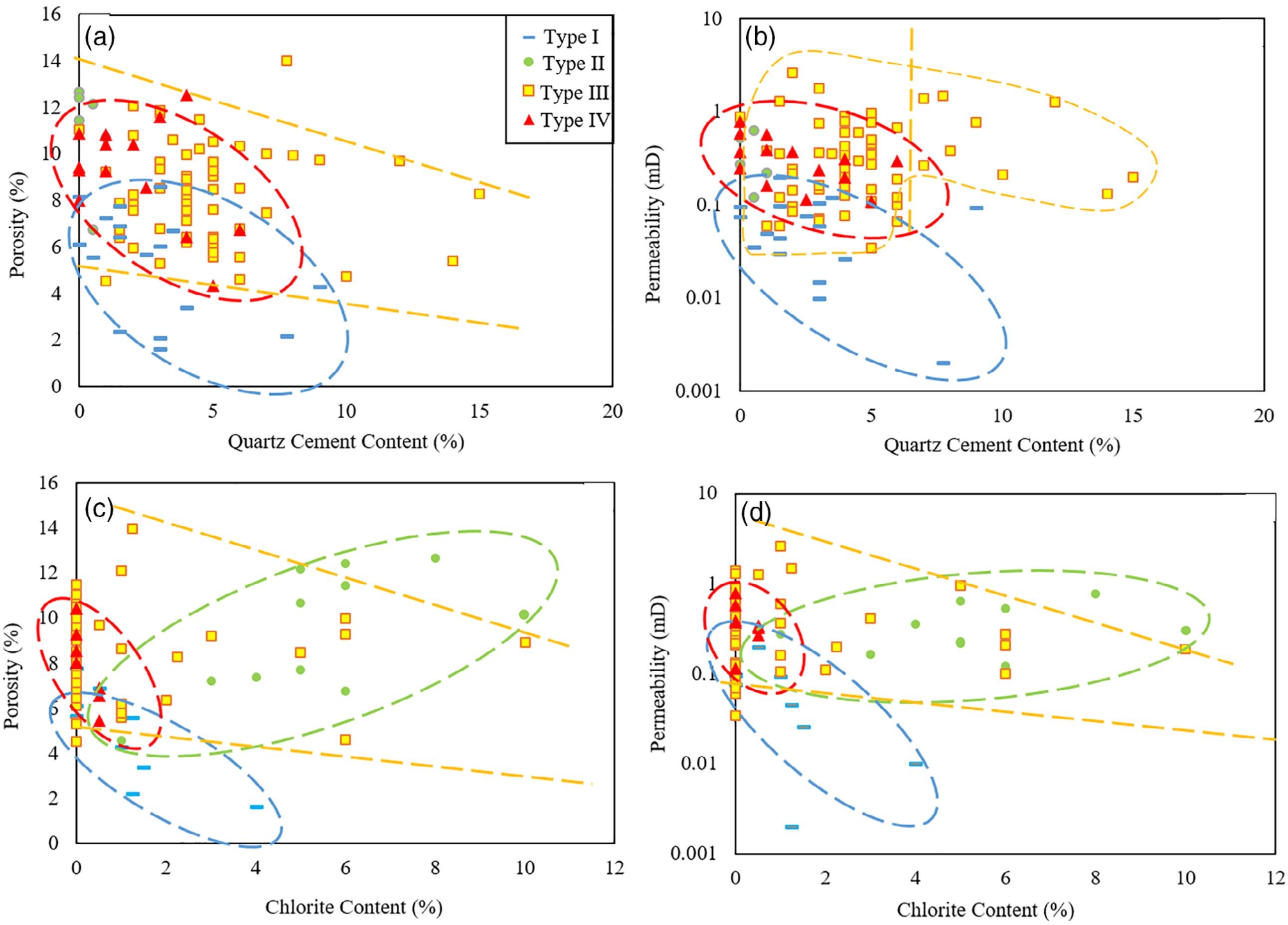

FIGURE 17 Relationships between diagenetic minerals (quartz and chlorite) and porosity (a and c) and permeability (b and d) of different types of sandstones [Colour figure can be viewed at wileyonlinelibrary.com]

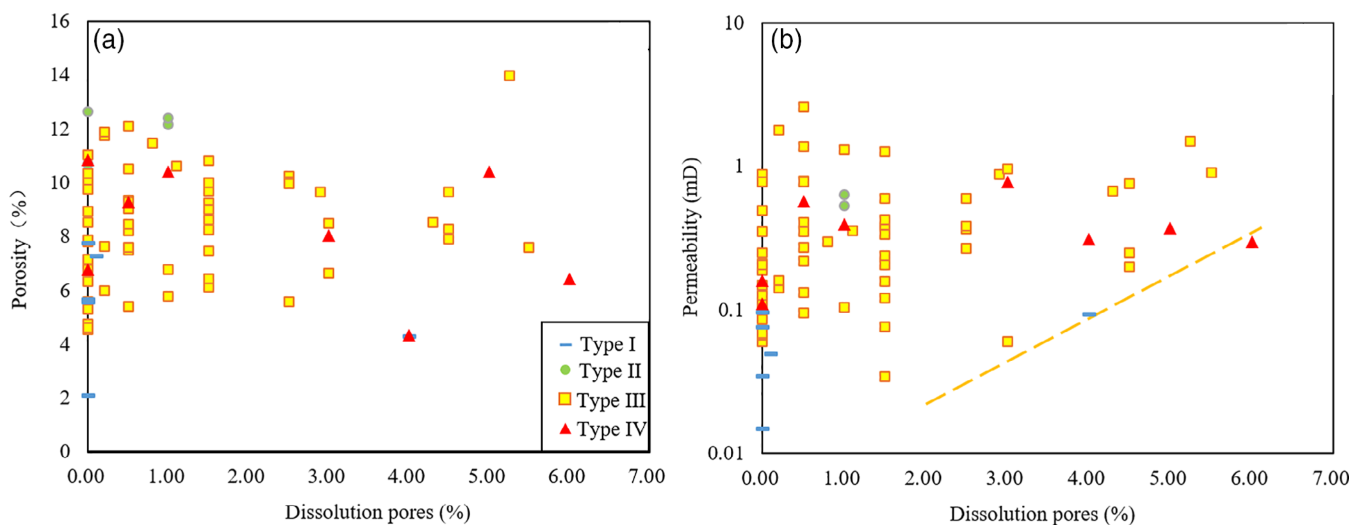

FIGURE 18 Relationship between dissolution pores and porosity (a) and permeability (b) in He8 sandstones [Colour figure can be viewed at wileyonlinelibrary.com]

positive correlation between grain-coating chlorites and reservoir quality in type II sandstones, indicating that the thickness of chlorite coating is not enough for blocking pores (Figure 17c,d). In contrast, when the chlorites develop as pore-filling, the porosity and permeability will decrease as the content of chlorites increase in other types of sandstones.

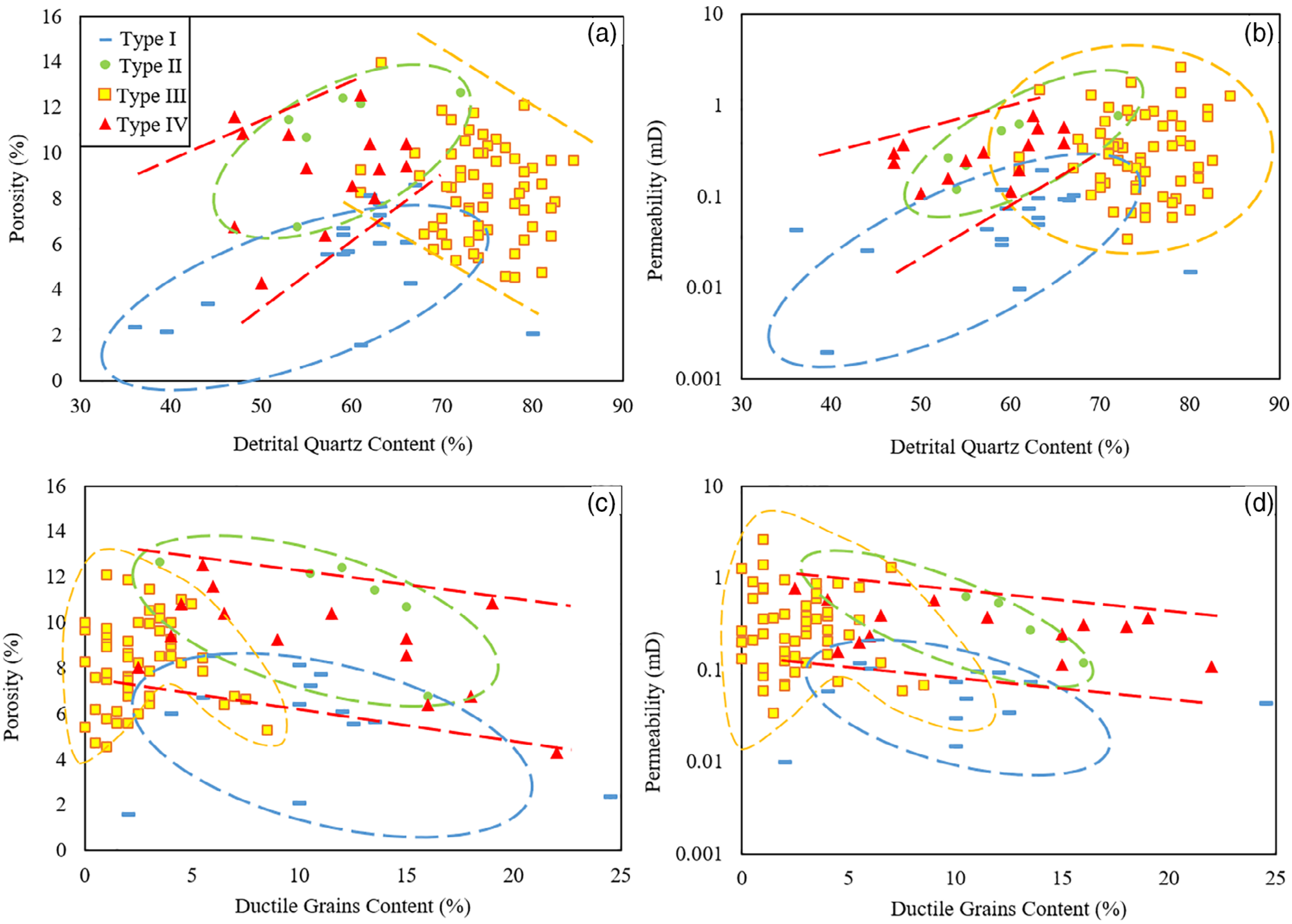

FIGURE 19 Relationships between components (detrital quartz and ductile grains) and porosity (a and c) and permeability (b and d) of different types of sandstones [Colour figure can be viewed at wileyonlinelibrary.com]

Dissolution is thought to be an important factor enhancing reservoir quality in coal-bearing strata (Li et al., 2017). However, the porosity and permeability do not show too much positive relationship with dissolution pores in He8 sandstone reservoirs (Figure 18a). This may be because the dissolution occurred mainly in the early meso-diagenesis stage, after which the pores will continue to be destroyed in late compaction. What is more, the secondary pores may be occupied by cementation such as quartz and calcite (Figure 6c,d). As discussed in previous studies, the dissolution in a closed system can only increase the porosity by about 0.7% (Li et al., 2017). Therefore, the dissolution can hardly improve reservoir quality in coal-bearing strata, unless the dissolution pores is over 3%, at this time the porosity and permeability can be improved slightly (Figure 18b).

5.4.2 | Control of petrographic characteristics on reservoir quality

The relationships between petrological characteristics and reservoir quality are the reflection of diagenesis on reservoir quality, which vary with the types of lithofacies. In general, fine-grained sandstones have lower reservoir qualities due to the tense mechanical compaction (Figure 9; Table 2). The content of detrital quartz shows significant correlation with reservoir quality in all types of sandstones, except type III (Figure 19a,b). For type III sandstones, more detrital quartz lead to more quartz overgrowth, which is the reason why porosity is greatly reduced and permeability changes little.

The relationships of ductile grains and reservoir quality also vary with the types of sandstones. As the ductile content increases, the porosity and permeability of all types of sandstones decrease, except type III (Figure 19c,d). Meanwhile, the reservoir quality of type IV sandstones does not decrease as fast as those in type I and type II sandstones. This is because the ductile grains can also produce an amount of dissolution pores, which contribute to the porosity and permeability. However, it shows in Figure 19c,d that when there are more ductile fragments, the porosity and permeability of type III sandstones increase first and then decrease, with a turning point at about 4%. This is because when the total content is under 4%, more ductile fragments lead to rapid decrease of quartz cementation (Figure 15c), thus increasing reservoir quality. When the total ductile content is over 4%, compaction will dominate during the burial process and more ductile fragments result in stronger compaction and lower porosity.

Although the inflection point of 4% may be different in other research areas, which may depend on the grain size, sorting, surface area of grains, and matrix contents, it is clear that how the ductile grains affect reservoir quality does not stay the same. Finding the quantitative and mutual relationship will help much in further exploration in tight sandstones in coal-bearing strata.

6 | CONCLUSIONS

1. Four types of sandstones according to various petrographic characteristics can be distinguished in Sulige area, including fine-grained sandstones (Type I), medium- to coarse-grained sandstones with abundant volcanic fragments (Type II), medium- to coarse-grained quartzarenite (Type III), and medium- to coarse-grained litharenite (Type IV). Type II sandstones are believed to be the best reservoirs for weaker compaction and less quartz cements during the diagenetic process.
2. Major sources of quartz cements are dissolution of feldspar and volcanic fragments, especially when the temperature is over 120°C and pressure solution at microstylolites, which are associated to the evolution of coals. The smectite to illite reaction only provides a little silica for early quartz cementation. The silica did not transport long distance and most precipitate in situ.
3. Petrographic characteristics control on the diagenesis of tight sandstones in coal-bearing strata: grain size together with detrital ductile account for the different degrees of compaction; more quartz grains can promote quartz cementation by providing more surface area as well as silica origin; volcanic grains and ductile fragments will inhibit quartz cement by reducing the nucleation of silica.
4. Compaction is the main reason for the porosity reduction after deposition, followed by quartz cement. The intense compaction is promoted by the dissolution of early calcite cements caused by coal evolution. The second-stage dissolution does not improve the reservoir quality much, due to the filling of diagenetic minerals.
5. The absence of feldspar enlarges the influence of quartz and rock fragment contents on reservoir quality in coal-bearing strata. For type III sandstones, the reservoir quality increase first and then decrease as the ductile content increase, which depends on the negative relationship of quartz cement and ductile contents. The turning point of 4% may change in other research areas, while the relationship can be helpful for further exploration.

ACKNOWLEDGEMENTS

This study was supported by the Major National Science and Technology Projects of China (Grant No. 2017ZX05009001) and the National Natural Science Foundation of China (Grant No. 41772101). Database was based on project that collaborated with Reach Institute of Sulige gas field, Changqing Oilfield Company, PetroChina. Engineer Ya Li, Yan Wang at the Reach Institute of Sulige gas field are also thanked for the help during the project.

PEER REVIEW

The peer review history for this article is available at https://publons.com/publon/10.1002/gj.4091.

DATA AVAILABILITY STATEMENT

Due to commercial restrictions, research data are not shared.

REFERENCES

Aase, N. E., & Walderhaug, O. (2005). The effect of hydrocarbons on quartz cementation: Diagenesis in the upper Jurassic sandstones of the Miller Field, North Sea, revisited. *Petroleum Geoscience*, *11*, 215–223.

Ajdukiewicz, J. M., & Lander, R. H. (2010). Sandstone reservoir quality prediction: the state of the art. *AAPG Bulletin*, *94*(8), 1083–1091.

Ajdukiewicz, J. M., & Larese, R. E. (2012). How clay grain coats inhibit quartz cement and preserve porosity in deeply buried sandstones: observations and experiments. *AAPG Bulletin*, *97*, 2091–2119.

Bao, H. P., Yang, Y. H., Wang, X. F., & Nan, J. X. (2007). Significance of syn-sedimentary volcanism for formation of sandstone reservoir of the Upper Paleozoic in Ordos Basin. *Journal of Palaeogeography*, *9*(4), 397–406.

Beard, D. C., & Weyl, P. K. (1973). Influence of texture on porosity and permeability of unconsolidated sand. *AAPG Bulletin*, *57*, 349–369.

Bi, M. W., Chen, S. Y., Zhou, Z. H., Zheng, G. Q., Zhang, M. L., Gao, L. X., … Liu, J. (2015). Densification modes of sandstone reservoir in the 8th member of the Lower Shihezi Formation, Permian, in Su-6 Area of Sulige Gas Field, Ordos Basin. *Geological Review*, *61*(03), 599–613.

Bjørlykke, K. (2011). Open-system chemical behaviour of Wilcox Group mudstones. How is large scale mass transfer at great burial depth in sedimentary basins possible? A discussion. *Marine and Petroleum Geology*, *28*, 1381–1382.

Bjørlykke, K. (2014). Relationships between depositional environments, burial history and rock properties. Some principal aspects of diagenetic process in sedimentary basins. *Sedimentary Geology*, *301*, 1–14.

Bjørlykke, K., & Egeberg, P. K. (1993). Quartz cementation in sedimentary basins. *AAPG Bulletin*, *77*, 1538–1548.

Bjørlykke, K., & Jahren, J. (2012). Open or closed geochemical systems during diagenesis in sedimentary basins: Constraints on mass transfer during diagenesis and the prediction of porosity in sandstone and carbonate reservoirs. *AAPG Bulletin*, *96*(12), 2193–2214.

Bjørlykke, K., Mo, A., & Palm, E. (1988). Modelling of thermal convection in sedimentary basins and its relevance to diagenetic reactions. *Marine and Petroleum Geology*, *5*(4), 338–351.

Carroll, A. R., Graham, S. A., & Smith, M. E. (2010). Walled sedimentary basins of China. *Basin Research*, *22*(1), 17–32.

Chen, S., Hou, Z., & Zhang, S. (2015). Diagenesis characteristics of volcanic material in He 8 Member, east block of Sulige Gas Field. *Duankuai Youqitian (Fault-Block Oil & Gas Field)*, *22*(2), 173–177.

Chuhan, F. A., Kjeldstad, A., Bjørlykke, K., & Høeg, K. (2002). Porosity loss in sand by grain crushing—Experimental evidence and relevance to reservoir quality. *Marine and Petroleum Geology*, *19*(1), 39–53.

Chuhan, F. A., Kjeldstad, A., Bjørlykke, K., & Høeg, K. (2003). Experimental compression of loose sands: Relevance to porosity reduction during burial in sedimentary basins. *Canadian Geotechnical Journal*, *40*(5), 995–1011.

Dutton, S., & Loucks, R. (2010). Diagenetic controls on evolution of porosity and permeability in lower Tertiary Wilcox sandstones from shallow to ultradeep (200–6700 m) burial, Gulf of Mexico Basin, U.S.A. *Marine and Petroleum Geology*, *27*(1), 69–81.

Fan, A. P., Wu, X. N., Wang, L., Zhang, C. Y., & Guo, J. F. (2016). Diagenetic mineral transformations and reservoir properties in the southwestern Sulige Gasfield, Ordos Basin, China. *Natural Gas Geoscience*, *27*(7), 1190–1201.

Fan, A. P., Yang, R. C., Lenhardt, N., Wang, M., Han, Z. Z., Li, J. B., & Zhao, Z. J. (2019). Cementation and porosity evolution of tight sandstone reservoirs in the Permian Sulige gas field, Ordos Basin (central China). *Marine and Petroleum Geology*, *103*, 276–293.

Fan, A. P., Yang, R. C., Li, J. B., Zhao, Z., & Van Loon, A. J. (2017). Siliceous cementation of chlorite coated grains in the Permian sandstone gas reservoirs, Ordos Basin. *Acta Geologica Sinica (English Edition)*, *91*(03), 1147–1114.

Fic, J., & Pedersen, P. K. (2013). Reservoir characterization of a "tight" oil reservoir, the middle Jurassic Upper Shaunavon Member in the Whitemud and Eastbrook pools, SW Saskatchewan. *Marine and Petroleum Geology*, *44*, 41–59.

Folk, R. L. (1980). *Petrology of sedimentary rocks*. Austin, Texas: Hemphill Publishing Company 182 p.

Giles, M., & De Boer, R. (1990). Origin and significance of redistributional secondary porosity. *Marine and Petroleum Geology*, *7*(4), 378–397.

Guo, Z., Jia, A. L., He, D. B., Tang, H. F., & Liu, Q. M. (2016). Characteristics of braided river sedimentary system zones in Sulige gas field, Ordos Basin. *Oil and Gas Geology*, *37*(2), 197–204.

Heald, M. T., & Renton, J. J. (1966). Experimental study of sandstone cementation. *Journal of Sedimentary Research*, *36*(4), 977–991.

Higgs, K., Zwingmann, H., Reyes, A., Funnell, R., & Higgs, K. E. (2007). Diagenesis, porosity evolution, and petroleum emplacement in tight gas reservoirs, Taranaki Basin, New Zealand. *Journal of Sedimentary Research*, *77*(12), 1003–1025.

Hodder, A., Naish, T., & Nelson, C. (1993). A two-stage model for the formation of smectite from detrital volcanic glass under shallow-marine conditions. *Marine Geology*, *109*(3), 279–285.

Hou, X., Zhu, Y., Chen, S., Wang, Y., & Liu, Y. (2020). Investigation on pore structure and multifractal of tight sandstone reservoirs in coal bearing strata using LF-NMR measurements. *Journal of Petroleum Science and Engineering*, *187*, 106757.

Hyodo, A., Kozdon, R., Pollington, A., & Valley, J. (2014). Evolution of quartz cementation and burial history of the Eau Claire Formation based on in situ oxygen isotope analysis of quartz overgrowths. *Chemical Geology*, *384*, 168–180.

Kim, J. C., Lee, Y., & Hisada, K. (2007). Depositional and compositional controls on sandstone diagenesis, the Tetori Group (Middle Jurassic-Early Cretaceous), central Japan. *Sedimentary Geology*, *195*(3/4), 183–202.

Lai, J., Wang, G., Chai, Y., Xin, Y., Wu, Q., Zhang, X., & Sun, Y. (2017). Deep burial diagenesis and reservoir quality evolution of high-temperature, high-pressure sandstones: Examples from Lower Cretaceous Bashijiqike Formation in Keshen area, Kuqa depression, Tarim basin of China. *AAPG Bulletin*, *101*(6), 829–862.

Lai, J., Wang, G., Ran, Y., & Zhou, Z. (2015). Predictive distribution of high quality reservoirs of tight gas sandstones by linking diagenesis to depositional facies: Evidences from Xu-2 sandstones in Penglai area of central Sichuan basin, China. *Journal of Natural Gas Science and Engineering*, *23*, 97–111.

Lai, J., Wang, G., Ran, Y., Zhou, Z., & Cui, Y. (2016). Impact of diagenesis on the reservoir quality of tight oil sandstones: The case of Upper Triassic Yanchang Formation Chang 7 oil layers in Ordos Basin, China. *Journal of Petroleum Science & Engineering*, *145*, 54–65.

Lai, J., Wang, G. W., Wang, S., Cao, J. T., Li, M., Pang, X. J., … Qin, Z. Q. (2018). Review of diagenetic facies in tight sandstones: Diagenesis, diagenetic minerals, and prediction via well logs. *Earth-Science Reviews*, *185*, 234–258.

Lai, J., Wang, G. W., Wang, Z. Y., Chen, J., Pang, X. J., Wang, S. C., … Fan, X. Q. (2018). A review on pore structure characterization in tight sandstones. *Earth-Science Reviews*, *177*, 436–457.

Lander, R. H., Larese, R. E., & Bonnell, L. M. (2008). Toward more accurate quartz cement models: The importance of euhedral versus non-euhedral growth rates. *AAPG Bulletin*, *92*(11), 1537–1563.

Lanson, B., Beaufort, D., Berger, G., Bauer, A., Cassagnabere, A., & Meunier, A. (2002). Authigenic kaolin and illitic minerals during burial diagenesis of sandstones: A review. *Clay Minerals*, *37*(1), 1–22.

Li, M., Guo, Y. H., Li, Z. F., & Wang, H. C. (2020). The diagenetic controls of the reservoir heterogeneity in the tight sand gas reservoirs of the Zizhou Area in China's east Ordos Basin: Implications for reservoir quality predictions. *Marine and Petroleum Geology*, *112*, 104088.

Li, Y., Chang, X., Yin, W., Wang, G. W., Zhang, J. L., Shi, B. B., … Mao, L. X. (2019). Quantitative identification of diagenetic facies and controls on reservoir quality for tight sandstones: A case study of the Triassic Chang 9 Oil Layer, Zhenjing Area, Ordos Basin. *Marine and Petroleum Geology*, *102*, 680–694.

Li, Y., Chang, X., Yin, W., Sun, T., & Song, T. (2017). Quantitative impact of diagenesis on reservoir quality of the Triassic Chang 6 tight oil sandstones, Zhenjing area, Ordos Basin, China. *Marine and Petroleum Geology*, *86*, 1014–1028.

Li, Y. J., Zhao, Y., Yang, R. C., Fan, A. P., & Li, F. P. (2010). Detailed sedimentary facies of a sandstone reservoir in the eastern zone of the Sulige gas field, Ordos Basin. *Mining Science and Technology (China)*, *20*(6), 891–903.

Liu, R. E., & Sun, F. J. (2002). An approach to the generating mechanism of secondary pores and pore evolution model of He8 gas layer in Suligemiao gas field. *Petroleum Exploration and Development*, *29*, 47–49.

Liu, R. E., Wu, H., Wei, X., Xiao, H. P., & Zhang, C. L. (2017). Anomaly distribution and genesis of feldspar in the 8th Member sandstone reservoir of Shihezi formation, Permian, Ordos basin. *Journal of China University of Mining and Technology*, *46*(1), 96–105.

Liu, Y., Hu, W., Cao, J., Wang, X., & Tang, Q. (2018). Diagenetic constraints on the heterogeneity of tight sandstone reservoirs: a case study on the upper Triassic Xujiahe Formation in the Sichuan Basin, Southwest China. *Marine and Petroleum Geology*, *92*, 650–669.

Lynch, F., Mack, L., & Land, L. (1997). Burial diagenesis of illite/smectite in shales and the origins of authigenic quartz and secondary porosity in sandstones. *Geochimica et Cosmochimica Acta*, *61*(10), 1995–2006.

Mansurbeg, H., Morad, S., Salem, A., Marfil, R., El-Ghali, M. A. K., Nystuen, J. P., … La Iglesia, A. (2008). Diagenesis and reservoir quality evolution of palaeocene deep-water, marine sandstones, the Shetland-Faroes Basin, British continental shelf. *Marine and Petroleum Geology*, *25*(6), 514–543.

Metwally, Y., & Chesnokov, E. (2012). Clay mineral transformation as a major source for authigenic quartz in thermo-mature gas shale. *Applied Clay Science*, *55*, 138–150.

Molenaar, N., Cyziene, J., & Sliaupa, S. (2007). Quartz cementation mechanisms and porosity variation in Baltic Cambrian sandstones. *Sedimentary Geology*, *195*(3), 135–159.

Morad, S., Al-Ramadan, K., Ketzer, J. M., & De Ros, L. F. (2010). The impact of diagenesis on the heterogenity of sandstone reservoirs: A review of the role of depositional facies and sequence stratigraphy. *AAPG Bulletin*, *94*(8), 1267–1309.

Nguyen, B. T., Jones, S. J., Goulty, N. R., Middleton, A. J., Grant, N., Ferguson, A., & Bowen, L. (2013). The role of fluid pressure and diagenetic cements for porosity preservation in Triassic fluvial reservoirs of the Central Graben, North Sea. *AAPG Bulletin*, *97*(8), 1273–1302.

Nie, J., Li, Y., Wei, Y. C., Wang, A. M., Jia, X., & Cao, D. Y. (2017). Contrastive analysis of Permo-Carboniferous and Jurassic coal reservoirs in northern Ordos basin. *Coal Geology of China*, *29*(11), 13–16.

Peltonen, C., Marcussen, Ø., Bjørlykke, K., & Jahren, J. (2009). Clay mineral diagenesis and quartz cementation in mudstones: The effects of smectite to illite reaction on rock properties. *Marine and Petroleum Geology*, *26*(6), 887–898.

Rahman, M., & Worden, R. (2016). Diagenesis and its impact on the reservoir quality of Miocene sandstones (Surma Group) from the Bengal Basin, Bangladesh. *Marine and Petroleum Geology*, *77*, 898–915.

Robinson, A., & Gluyas, J. (1992). Duration of quartz cementation in sandstones, North Sea and Haltenbanken Basins. *Marine and Petroleum Geology*, *9*, 324–327.

Shoval, S. (2004). Deposition of volcanogenic smectite along the south-eastern Neo-Tethys margin during the oceanic convergence stage. *Applied Clay Science*, *24*(3), 299–311.

Shuai, Y. H., Zhang, S. C., Gao, Y., Lu, H., Chen, J. P., Mi, J., … Guo, Y. (2013). Effect and quantitative evaluation of CO_2 derived from organic matter in coal on the formation of tight sandstone reservoirs - Effect and quantitative evaluation of CO_2 derived from organic matter in coal on the formation of tight sandstone reservoirs. *Science China Earth Sciences*, *05*, 756–762.

Srodon, J. (1999). Nature of mixed-layer clays and mechanisms of their formation and alteration. *Annual Review Earth Planetary Science*, *27*, 19–53.

Storvoll, V., Bjørlykke, K., Karlsen, D., & Saigal, G. (2002). Porosity preservation in reservoir sandstones due to grain-coating illite: A study of the Jurassic Garn Formation from the Kristin and Lavrans fields, offshore Mid-Norway. *Marine and Petroleum Geology*, *19*(6), 767–781.

Thyberg, B., Jahren, J., Winje, T., Bjørlykke, K., Faleide, J., & Marcussen, O. (2010). Quartz cementation in Late Cretaceous mudstones, northern North Sea: Changes in rock properties due to dissolution of smectite and precipitation of micro-quartz crystals. *Marine and Petroleum Geology*, *27*(8), 1752–1764.

Tian, M., Omre, H., & Xu, H. (2020). Inversion of well logs into lithology classes accounting for spatial dependencies by using hidden Markov models and recurrent neural networks. *Journal of Petroleum Science and Engineering*, *196*, 107598.

Walderhaug, O. (1994). Temperatures of quartz cementation in Jurassic sandstones from the Norwegian continental shelf-evidence from fluid inclusions. *Journal of Sedimentary Research*, *64*(2a), 311–323.

Walderhaug, O. (2000). Modeling quartz cementation and porosity in Middle Jurassic Brent Group sandstones of the Kvitebjørn Field, Northern North Sea. *AAPG Bulletin*, *84*, 1325–1339.

Wang, G., Chang, X., Yin, W., Li, Y., & Song, T. (2017). Impact of diagenesis on reservoir quality and heterogeneity of the Upper Triassic Chang 8 tight oil sandstones in the Zhenjing area, Ordos Basin, China. *Marine and Petroleum Geology*, *83*, 84–96.

Wang, G. W., Hao, F., Chang, X. C., Lan, C. J., Li, P. P., & Zou, H. Y. (2017). Quantitative analyses of porosity evolution in tight grainstones: A case study of the Triassic Feixianguan formation in the Jiannan gas field, Sichuan Basin, China. *Marine and Petroleum Geology*, *86*, 259–267.

Wang, T., Hou, M. C., Wang, W. K., Wang, F., Wu, H., & Su, Z. T. (2011). Sand body configuration of sequence stratigraphic framework of the 8^{th} Member of the Permian Lower Shihezi Fm in Zhao 30 wellblock, eastern Sulige Gas Field, Ordos Basin. *Natural Gas Industry*, *34*(7), 27–33.

Wang, X. P., & Mou, C. L. (2013). Diagenesis and diagenetic facies of reservoir in He8 section of Shihezi Formation in east II part of Sulige gas field. *Natural Gas Geoscience*, *24*(04), 678–689.

Worden, R. H., Mayall, M., & Evans, I. J. (2000). The effect of ductile-lithic sand grains and quartz cement on porosity and permeability in Oligocene and lower Miocene Clastics, South China Sea: Prediction of reservoir quality. *AAPG Bulletin*, *84*, 534–359.

Worden, R. H., & Morad, S. (2000). Quartz cementation in oil field sandstones: A review of the key controversies. *Special Publication-International Association of Sedimentologists*, *29*, 1–20.

Xi, K., Cao, Y., Jahren, J., Zhu, R., Bjørlykke, K., Zhang, X., … Hellevang, H. (2015). Quartz cement and its origin in tight sandstone reservoirs of the Cretaceous Quantou formation in the southern Songliao basin, China. *Marine and Petroleum Geology*, *66*(4), 748–763.

Xi, S. L., Liu, X., & Meng, P. (2015). Exploration practices and prospect of Upper Paleozoic giant gas fields in the Ordos Basin. *Natural Gas Industry B*, *2*(5), 430–439.

Xi, S. L., Wang, H. C., & Qin, B. P. (2002). Analysis of the material sources of ShanXi formation and ShiHezi formation in north Erduosi Basin. *Natural Gas Industry*, *22*(2), 21–24.

Yang, H., Fu, J., Liu, X., & Fan, L. (2012). Formation conditions and exploration techniques of Sulige large tight sandstone gas reservoir. *Acta Petrolei Sinica*, *33*(1), 27–36.

Yang, H., Fu, J., Wei, X., & Liu, X. (2008). Sulige field in the ordos basin: geological setting, field discovery and tight gas reservoirs. *Marine and Petroleum Geology*, *25*(4), 387–400.

Yang, H., & Liu, X. (2014). Progress in coal gas exploration of Paleozoic in Ordos basin. *Petroleum Exploration and Development*, *44*, 129–137.

Yang, H., Yang, Y., Shi, X. H., & Yin, P. (2007). Influence of the late Paleozoic volcanic activity on the sandstone reservoir in the interior of Ordos Basin. *Acta Sedimentologica Sinica*, *25*, 526–534.

Yang, R., Fan, A., Han, Z., & Wang, X. (2012). Diagenesis and porosity evolution of sandstone reservoirs in the East II part of Sulige gas field, Ordos Basin. *International Journal of Mining Science and Technology*, *22*(3), 311–316.

Yang, R., Fan, A., Van Loon, A. J., Han, Z., & Wang, X. (2014). Depositional and diagenetic controls on sandstone reservoirs with low porosity and low permeability in the Eastern Sulige gas field, China. *Acta Geologica Sinica*, *88*(5), 1513–1534.

Yang, R., Jin, Z., Van Loon, A. J., Han, Z., & Fan, A. (2017). Climatic and tectonic controls of lacustrine hyperpycnite origination in the late Triassic Ordos basin, central China: Implications for unconventional petroleum development. *AAPG Bulletin*, *101*, 95–117.

Yu, Y., Lin, L., Zhai, C., Chen, H., Wang, Y., Li, Y., & Deng, X. (2019). Impacts of lithologic characteristics and diagenesis on reservoir quality of the 4th member of the Upper Triassic Xujiahe Formation tight gas sandstones in the western Sichuan Basin, southwest China. *Marine and Petroleum Geology*, *107*, 1–19.

Yuan, G., Cao, Y., Gluyas, J., Li, X., Xi, K., Wang, Y., … Oxtoby, N. H. (2015). Feldspar dissolution, authigenic clays, and quartz cements in open and closed sandstone geochemical systems during diagenesis: Typical examples from two sags in Bohai Bay Basin, East China. *AAPG Bulletin*, *99*(11), 2121–2154.

Zhao, J., Zhang, W., Li, J., Cao, Q., & Fan, Y. (2014). Genesis of tight sand gas in the Ordos Basin, China. *Organic Geochemistry*, *74*, 76–84.

Zhen, J. M., & Feng, X. Y. (1997). Reservoir characteristics and diagenetic model of sandstone intercalated in coal-bearing strata (acid water medium). *Acta Petrolei Sinica*, *18*(4), 19–24.

Zhu, X. M., Liu, C. L., Zhong, D. K., & Han, X. F. (2009). Diagenesis and their succession of gas-bearing and non-gas-bearing reservoirs in the Sulige gas field of Ordos Basin, China. *Acta Geologica Sinica-English Edition*, *83*(6), 1202–1213.

Zou, C., Yang, Z., Huang, S., Ma, F., Sun, Q., Li, F., … Tian, W. (2019). Resource types, formation, distribution and prospects of coal-measure gas. *Petroleum Exploration and Development*, *46*(3), 451–462.

Zou, C., Zhu, R., Liu, K., Su, L., Bai, B., Zhang, X., … Wang, J. (2012). Tight gas sandstone reservoirs in China: Characteristics and recognition criteria. *Journal of Petroleum Science & Engineering*, *88-89*, 82–91.

How to cite this article: Liu Z, Wu S, Li J, et al. Impact of petrographic characteristics on reservoir quality of tight sandstone reservoirs in coal-bearing strata: A case study in Lower Permian Shihezi Formation in northern Ordos Basin, China. *Geological Journal*. 2021;56:3097–3117. https://doi.org/10.1002/gj.4091